AD________________

Award Number: DAMD17-03-1-0004

TITLE: Oral Administration of N-Acetyl-D-Glucosamine Polymer Particles Down-Regulates Airway Allergic Responses

PRINCIPAL INVESTIGATOR: Yoshimi Shibata, Ph.D.

CONTRACTING ORGANIZATION: Florida Atlantic University
Boca Raton FL 33431-0991

REPORT DATE: March 2007

TYPE OF REPORT: Annual

PREPARED FOR: U.S. Army Medical Research and Materiel Command
Fort Detrick, Maryland 21702-5012

REPORT DOCUMENTATION PAGE

Form Approved
OMB No. 0704-0188

1. REPORT DATE *(DD-MM-YYYY)*
01-03-2007

2. REPORT TYPE
Annual

3. DATES COVERED *(From - To)*
24 Feb 06 – 23 Feb 07

4. TITLE AND SUBTITLE
Oral Administration of N-Acetyl-D-Glucosamine Polymer Particles Down-Regulates Airway Allergic Responses

5a. CONTRACT NUMBER

5b. GRANT NUMBER
DAMD17-03-1-0004

5c. PROGRAM ELEMENT NUMBER

6. AUTHOR(S)
Yoshimi Shibata, Ph.D.

E-Mail: yshibata@fau.edu

5d. PROJECT NUMBER

5e. TASK NUMBER

5f. WORK UNIT NUMBER

7. PERFORMING ORGANIZATION NAME(S) AND ADDRESS(ES)

Florida Atlantic University
Boca Raton FL 33431-0991

8. PERFORMING ORGANIZATION REPORT NUMBER

9. SPONSORING / MONITORING AGENCY NAME(S) AND ADDRESS(ES)
U.S. Army Medical Research and Materiel Command
Fort Detrick, Maryland 21702-5012

10. SPONSOR/MONITOR'S ACRONYM(S)

11. SPONSOR/MONITOR'S REPORT NUMBER(S)

12. DISTRIBUTION / AVAILABILITY STATEMENT
Approved for Public Release; Distribution Unlimited

13. SUPPLEMENTARY NOTES - Original contains colored plates: ALL DTIC reproductions will be in black and white.

14. ABSTRACT:
This is an annual report of the 4th grant year. PI and 2 Research Associates moved to the current Institute in 2003 from East Carolina University. The project was re-started in December 2004 with approval of no-cost extension until 5/23/2008. In this grant period, we found that administration of chitin particles resulted in less likely inhibit the production of IL-10. Although chitin particles induce peritoneal macrophages catalytically active COX-2 in vitro, intraperitoneal administration induces peritoneal macrophages catalytically inactive COX-2. COX-2, cyclooxygenase, is necessary enhancing prostaglandin E2 (PGE2) release. Both IL-10 and PGE2 enhance allergic responses. We have also planned to establish a method producing chitin particles at 500 – 1,000 gram per batch.

15. SUBJECT TERMS
Childhood asthma, N-acetyl-D-glucosamine polymer, IL-12, GATA-3, T-bet, macrophages, airway hyperreactivity

16. SECURITY CLASSIFICATION OF:			17. LIMITATION OF ABSTRACT	18. NUMBER OF PAGES	19a. NAME OF RESPONSIBLE PERSON USAMRMC
a. REPORT	b. ABSTRACT	c. THIS PAGE			19b. TELEPHONE NUMBER *(include area code)*
U	U	U	UU	71	

Table of Contents

INTRODUCTION:
This annual report includes a brief summary of the 4th year research and related activities supported by DAMD17-03-1-0004.

This project funded by DOD DAMD17-03-1-0004 was initiated at East Carolina University on February 24, 2003. PI and two research associates moved to the current institute, Florida Atlantic University (FAU), on September 30, 2003. The transfer of grantee institute was approved on December 1, 2004. Since then, the project has re-started with no-cost extension until May 23, 2008. Two postdoctoral research associates, Shoutaro Tsuji, Ph.D. and Makiko Y. Tsuji, DVM, Ph.D. joined the laboratory and conducted this project starting in April 2005 until December 2006. Tsutomu Shinohara, M.D., Ph.D., a pulmonary physician/scientist, has joined in May 2006 and conducted the project. Harni Patel, a graduate student, has joined in January 2007.

BODY:
Task 1: To determine if oral administration of 1 – 4 μm particles of chitin will down-regulate airway hyperreactivity (AHR) and GATA-3 levels as a measure of Th2 responses, and enhance T-bet levels as a measure of Th1 responses in the lungs of mice that are sensitized with ragweed allergens.
a. Establish the effects of dose response of chitin particles (Months 1 – 4).
b. Establish therapeutic/prophylactic effects of chitin (Months 4 – 9).
c. Determine duration of chitin treatments (Months 8 - 12).

This has been completed.

Task 2: To determine if the effects of 1 – 4 μm particles of chitin on endogenous IL-12- or IFNγ- mediated down-regulation of airway allergic responses will be greater than those of HK-BCG, ODN-CpG or an equal number of particles of 1 – 10 μm chitin.

a. Establish comparative studies on the effects of 1 – 4 μm chitin, 1 – 10 μm chitin, HK-BCG and ODN-CpG (Months 12 - 24).

b. Study if endogenous IL-12 or IFNγ is required for the chitin-induced down-regulation of GATA-3-mediated allergic responses (Months 24 – 40).

We found that splenic PGE_2-M∅ down-regulate the activity of HK-BCG as a Th1 adjuvant. A summary of the findings is below.

Previous studies showed that increased PGE_2 release by splenic F4/80$^+$ COX-2$^+$ macrophages (M∅) isolated from mice treated with mycobacterial components plays a major role in the regulation of immune responses is associated with unique immunoregulation. Normal splenic M∅, when pre-treated *in vitro* with LPS and IFNγ, express COX-1 and COX-2 within 1 day but release minimal amounts of PGE_2 following elicitation with calcium ionophore A23187. In this study, to further characterize requirements for the development of PGE_2-releasing M∅ (PGE_2-M∅), C57Bl/6 (WT) and IL- 10$^{-/-}$ mice were treated ip with heat-killed (HK) *Mycobacterium bovis* BCG. One day following injection, we found that COX-2 was induced in splenic M∅ in an IL-10-independent manner. However, following *ex vivo* elicitation, these M∅ showed little or no increase in PGE_2 biosynthesis. In sharp contrast, 14 days after HK-BCG treatment, PGE_2 release by splenic M∅ increased as much as 10 fold in an IL-10-dependent manner. To further determine the source of the 14-day splenic PGE_2-M∅, we established a bone marrow chimera in which bone marrow cells were transfused from green fluorescent protein (GFP)-transgenic donors to WT mice. Both donors and recipients were treated with HK-BCG simultaneously and bone marrow transfusion was performed on days 1 and 2. On day 14 after BCG treatment, a significant number of spleen cells co-expressed COX-2 and GFP. Our results indicate that on day 1 after BCG treatment, the presence of COX-2 alone is not sufficient to induce PGE_2 biosynthesis by splenic M∅ and that bone marrow-derived M∅ may contribute to increased PGE_2 production by 14 days after BCG treatment in an IL-10 dependent manner.

Task 3: To determine if M∅ will phagocytose more particles and produce more IL-12 in response to 1 – 4 μm chitin compared to 1 – 10 μm chitin.

a. Determine if M∅ treated with 1 – 4 μm chitin particles phagocytose more particles than when treated with an equivalent number of 1 – 10 μm chitin particles (Months 41 – 44).

b. Determine if 1 – 4 μm chitin particles induce more production of IL-12 than an equivalent number of 1 – 10 μm chitin particles (Months 45 – 48).

Cellular events of phagocytosis that are associated with chitin-induced production of anti- and pro-inflammatory cytokines were characterized. A manuscript, "Phagocytosis of *N*-acetyl-D-glucosamine particles, a Th1 adjuvant, results in MAPK activation and TNF-α, but not IL-10, production," was published by Cellular Immunology. A summary of these findings is below.

A practical Th1 adjuvant should induce Th1 cytokines (IL-12, IL-18 and TNF-α) but not the Th2 cytokine IL-10, an inhibitor of Th1 responses. In this study, phagocytosis of *N*-acetyl-D-glucosamine polymer (chitin) particles by RAW264.7 macrophage-like cells resulted in phosphorylation of MAPK (p38, Erk1/2 and JNK) and production of relatively high levels of TNF-α and COX-2 with increased PGE_2 release. Similar results were observed in response to bacterial Th1 adjuvants (oligonucleotides with CpG motifs and mycobacterial components) and endotoxin. However, these bacterial components also induced a large amount of IL-10. Chitin particles, in contrast, induced only minimal levels of IL-10, although the production of high levels of PGE_2 and TNFα and the activation of MAPK's are potentially positive signals for IL-10 production. Thus, our results indicate that in macrophages chitin particles act as a unique Th1 adjuvant without inducing increased production of IL-10.

To further investigate the mechanisms of phagocytosis-mediated MØ activation, RAW264.7 MØ were depleted of cellular cholesterol by methyl-β-cytodextrin (MBCD) followed by chitin particle stimulation. We found that neither levels of MØ binding chitin particles nor phagocytosing chitin particles within 20 min were altered by MBCD treatment. The kinetics and extent of chitin-induced phosphorylation of MAPK were accelerated and enhanced, respectively, by MBCD in a dose dependent manner. Chitin particle-induced TNF-α production, cyclooxygenase 2 expression, and prostaglandin E_2 release were enhanced by MBCD. However, in neither MBCD- nor saline- treated MØ, chitin particles induce IL-10 production. As a comparison control, CpG-ODN-induced MØ activation measured by MAPK activation, TNFα production, COX-2-mediated PGE_2 biosynthesis and IL-10 production is relatively insensitive to MBCD treatment. Our study indicated that phagocytosis-mediated MØ activation uniquely involves a mechanism depending on cellular cholesterol levels.

KEY RESEARCH ACCOMPLISHMENTS:

1. Establishment of cellular mechanisms underlying phagocytosis of chitin particles and production of anti-inflammatory cytokines by macrophages.
2. Establishment of the chitin Th1 adjuvant which inhibits IL-10, a Th2 cytokine, production.
3. Finding a novel mechanism underlying chitin particles down-regulating the activities of COX-2 in a post-translational regulation.
4. Establishment of characterization of splenic PGE_2-releasing macrophages which induce a Th1-to-Th2 shift of immune responses.
5. Establishment of a method possibly producing chitin particles at 500 – 1,000 gram per batch.

REPORTABLE OUTCOMES:

<u>Paper Published</u>

Van Scott MR, JL Hooker, D Ehrmann, Y Shibata, C Kukoly, K Salleng, G Westergaard, A Sandrasagra, J Nyce. Dust mite-induced asthma in Cynomolgus monkeys. *J Appl Physiol 96:1433-1444, 2003. Task 2.*

Shibata Y, A Nishiyama, H Ohata, J Gabbard, QN Myrvik, RA Henriksen. Differential effects of IL-10 on prostaglandin H synthase-2 expression and prostaglandin E_2 biosynthesis between spleen and bone marrow macrophages. *J. Leuko. Biol. 77:544-551, 2005.* Tasks 2 and 3.

Shibata Y, Henriksen RA, Honda I, Nakamura RM, Myrvik QN. Splenic PGE2-releasing macrophages regulate Th1 and Th2 immune responses in mice treated with heat-killed BCG. *J Leukoc Biol 78, 1281-1290, 2005.* Task 2.

Shibata Y. Radiosensitive macrophages and immune responses --- Prostaglandin E_2-releasing macrophages induce a Th1-to-Th2 shift of immune responses in chronic inflammation ---*Proceeding of "International Symposium on Low-Dose Radiation Exposures and Bio-Defense System.* Page 5, 2006. Task 2.

Shibata Y, J Gabbard, M Yamashita, S Tsuji, M Smith, A Nishiyama, RA Henriksen, QN Myrvik. Heat-killed BCG induces biphasic cyclooxygenase-2^+ splenic macrophage formation --- role of IL-10 and bone marrow precursors. *J Leukocyte Biol 80:590-598, 2006.* Task 2.

Nishiyama, A, S Tsuji, M Yamashita, RA Henriksen, QN Myrvik, Y Shibata. Phagocytosis of *N*-acetyl-D-glucosamine particles, a Th1 adjuvant, results in MAPK activation and TNF-α, but not IL-10, production. *Cell Immunol 239:103 – 112, 2006.* Tasks 1a, 3a and 3b.

Shibata Y, H Ohata, M Yamashita, S Tsuji, JF Bradfield, RA Hendrickson, A Nishiyama, QN Myrvik. Immunologic response enhances atherosclerosis -- Th1-to-Th2 shift and calcified atherosclerosis in BCG-treated apolipoprotein $E^{-/-}$ mice. *Translational Research 149:62-69, 2007.* Task 2.

<u>Manuscript in press</u>

Yamashita M, A Nishiyama, QN Myrvik, RA Henriksen, S Tsuji, Y Shibata. Differential subcellular localization of COX-2 by macrophages phagocytosing *Mycobacterium bovis* BCG in vivo. *Am J Physiol (Cell Physiology)* (in press).

Tsuji S, M Yamashita, A Nishiyama, Z. Li, QN Myrvik, RA Henriksen, Y Shibata. Differential structure and activity between human and mouse intelectin-1: human intelectin-1 is a disulfide-linked oligomer, whereas mouse homologue is a monomer. *Glycobiology* (Accepted in revision).

<u>Manuscript submitted or in preparation</u>

Shibata, Y, P Vos, QN Myrvik. Neutrophils from BCG-immunized mice enhance innate immunity against lethal challenges of *Listeria monocytogenes*. Submitted for publication. Task 2.

Nishiyama A, MY Tsuji, S Tsuji, RA Henriksen, QN Myrvik, Y Shibata. Cellular Cholesterol Depletion Enhances Chitin Phagocytosis-Induced Macrophage Activation. Abstract was presented at AAI Meeting at Boston in May 2006. Tasks 1 and 3.

Munim A, A Nishiyama, S Tsuji, M Yamashita, QN Myrvik, Y Shibata. A novel oral agent activates macrophages and down-regulates Th2 allergic responses. Abstract was presented at American Thoracic Society Meeting at San Diego in May 2006. Task 1.

Presentations

Yamashita M, A Nishiyama, QN Myrvik, RA Henriksen, S Tsuji, Y Shibata. Heat-killed BCG induces biphasic cyclooxygenase-2 $(COX\text{-}2)^+$ splenic macrophage formation – differential intracellular compartmentalization of COX-2 correlates with PGE_2 biosynthesis. Abstract was presented at AAI Meeting at Boston in May 2006. Task 2.

Tsuji S, M Yamashita, A Nishiyama, Y Shibata. Molecular structure of human and mouse interlectin-1 and comparison of binding to a mycobacterial galactofuranosyl residue.
Abstract was presented at AAI Meeting at Boston in May 2006. Task 2.

Shinohara T, M Yamashita, A Nishiyama, S Tsuji, QN Myrvik, RA Henriksen , Y Shibata. Differential regulation of cyclooxygenase (COX) isoforms in alveolar and peritoneal macrophages from heat-killed *Mycobacterium bovis* BCG treated mice. Abstract will be presented at AAI Meeting at Miami in May 2007.

"A novel chitin Th1 adjuvant activates macrophages down-regulating Th2 allergic responses," the CDMRP's Military Health Research Forum (MHRF, sponsored by DOD), San Juan, Puerto Rico, 5/1 – 5/4/06.

"Host factors for infections and interventions," the 31st Annual Educational Conference and Meeting of the Florida Professionals in Infection Control (FPIC). Orlando, FL, 9/13/06.

US Paatent

US Provisional Patent Application, "Chitin micro-particles as an adjuvant" by Yoshimi Shibata and Quentin N. Myrvik, 6/16/06, through FAU OTT. APPLICATION NO. 60/814,382

EMPLOYMENT:

Two Postdoctoral Research Associates, Shoutaro Tsuji, Ph.D. and Makiko Y. Tsuji, DVM, Ph.D., joined the laboratory and conduct this project starting in April 2005 until December 2006. Tsutomu Shinohara, M.D., Ph.D., Research Associate Professor and a pulmonary specialist joined and performed animal studies in this project since May 2006. Harni Patel, a graduate student, has joined in January 2007.

CONCLUSIONS:

The neonates and young children are more susceptible than the young to infections and frequently develop asthmatic problems (1, 2). The mechanism by which these populations become immunocompromised appears to be an altered regulation of immunity and not simple immune deficiency. It is likely that macrophages in these immunocompromised populations become hypofunctional with excessive production of PGE_2 and IL-10, both of which enhance allergic Th2 responses. Our studies clearly demonstrated that administration of chitin particles resulted in blocking the production of IL-10 and COX-2/PGE_2biosynthesis. In sharp contrast, bacterial Th1 adjuvants (heat-killed *Mycobacteirum bovis* BCG, CpG-ODN) and endotoxin (LPS) enhances both IL-10 production and PGE_2 release (3-5). Thus chitin may be the most potent Th1 adjuvant presently available and is an attractive immunomodulator for allergic asthma.

A composition and method for the preparation of micro-particles of chitin (a naturally occurring polymer of N-acetyl-D-glucosamine), the characterization of chitin micro-particles as an immune adjuvant and the use of chitin micro-particles to enhance protective immunity against intracellular infectious agents and diseases as well as to inhibit allergic responses and diseases. We have established a method to produce bioactive chitin micro-particles at scales of 0.1 – 1 gram. To perform Phase I clinical trials, a large scale of production line at 500 – 1,000 gram levels is needed. We plan to establish the scale-up method in collaboration with Yaizu Suisankagaku Industry Co. Ltd (YSK), Shizuoka, Japan, leading similar chitin products.

REFERENCES:

1. van Benten, I. J., C. M. van Drunen, L. P. Koopman, B. C. van Middelkoop, W. C. Hop, A. D. Osterhaus, H. J. Neijens, and W. J. Fokkens. 2005. Age- and infection-related maturation of the nasal immune response in 0-2-year-old children. *Allergy* 60:226-232.
2. Blahnik, M. J., R. Ramanathan, C. R. Riley, and P. Minoo. 2001. Lipopolysaccharide-induced tumor necrosis factor-alpha and IL-10 production by lung macrophages from preterm and term neonates. *Pediatr Res* 50:726-731.
3. Shibata, Y., R. A. Henriksen, I. Honda, R. M. Nakamura, and Q. N. Myrvik. 2005. Splenic PGE2-releasing macrophages regulate Th1 and Th2 immune responses in mice treated with heat-killed BCG. *J Leukoc Biol* 78:1281-1290.
4. Shibata, Y., J. Gabbard, M. Yamashita, S. Tsuji, M. Smith, A. Nishiyama, R. A. Henriksen, and Q. N. Myrvik. 2006. Heat-killed BCG induces biphasic cyclooxygenase 2+ splenic macrophage formation--role of IL-10 and bone marrow precursors. *J Leukoc Biol* 80:590-598.
5. Nishiyama, A., S. Tsuji, M. Yamashita, R. A. Henriksen, Q. N. Myrvik, and Y. Shibata. 2006. Phagocytosis of N-acetyl-d-glucosamine particles, a Th1 adjuvant, by RAW 264.7 cells results in MAPK activation and TNF-alpha, but not IL-10, production. *Cell Immunol* 239:103-112.

APPENDICES:

Appendix I: Shibata Y, H Ohata, M Yamashita, S Tsuji, JF Bradfield, RA Hendrickson, A Nishiyama, QN Myrvik. Immunologic response enhances atherosclerosis -- Th1-to-Th2 shift and calcified atherosclerosis in BCG-treated apolipoprotein $E^{-/-}$ mice. *Translational Research 149:62-69, 2007.* Task 2.

Appendix II: Yamashita M, A Nishiyama, QN Myrvik, RA Henriksen, S Tsuji, Y Shibata. Differential subcellular localization of COX-2 by macrophages phagocytosing *Mycobacterium bovis* BCG in vivo. *Am J Physiol (Cell Physiology)* (in press).

American Journal of Physiology: Cell Physiology

Differential subcellular localization of COX-2 in macrophages phagocytosing heat-killed *Mycobacterium bovis* BCG |

Journal:	*AJP: Cell Physiology*
Manuscript ID:	C-00346-2006.R2
Manuscript Type:	Original Article
Date Submitted by the Author:	n/a
Complete List of Authors:	Yamashita, Makiko; Florida Atlantic University, Biomedical Sciences Tsuji, Shoutaro; Florida Atlantic University, Biomedical Sciences Nishiyama, Akihito; Florida Atlantic University, Biomedical Sciences Myrvik, Quentin Henriksen, Ruth Ann; East Carolina University, Physiology Shibata, Yoshimi; Florida Atlantic University, Biomedical Sciences
Key Words:	cyclooxygenase, prostaglandin E2, macrophage, phagocytosis, BCG

Differential subcellular localization of COX-2 in macrophages phagocytosing heat-killed *Mycobacterium bovis* BCG

Makiko Yamashita[1], Shoutaro Tsuji[1], Akihito Nishiyama[1], Quentin N. Myrvik[3], Ruth Ann Henriksen[2] Yoshimi Shibata[1]

[1]Department of Biomedical Sciences, Florida Atlantic University, Boca Raton, FL 33431-0991, [2]Department of Physiology, Brody School of Medicine at East Carolina University, Greenville, NC 27834, [3]Palmeto Dr, Caswell Beach, NC 28465

Address correspondence and reprint requests to Yoshimi Shibata, Ph.D., Department of Biomedical Sciences, Florida Atlantic University, 777 Glades Rd., P.O. Box 3091, Boca Raton, FL 33431-0991. Telephone number (561) 297-0606, Fax number (561) 297-2221, E-mail yshibata@fau.edu

Running head: Phagocytosis, mycobacteria and catalytically inactive COX-2

ABSTRACT

Cyclooxygenase-2 (COX-2)-mediated prostaglandin E_2 (PGE_2) biosynthesis by macrophages (M∅) down-regulates microbicidal activities in innate and acquired immune responses against intracellular bacteria. Previous studies in mice showed that intraperitoneal administration of heat-killed *Mycobacterium bovis* bacillus Calmette-Guérin (HK-BCG) resulted in induction of splenic PGE_2-releasing M∅ (PGE_2-M∅) in 7 – 14 days. In contrast, HK-BCG induced catalytically inactive COX-2 at relatively high levels in the M∅ within 1 day. In the present study, we found that COX-2 was localized subcellularly in the nuclear envelope (NE) on days 7 and 14 after HK-BCG treatment, whereas day 1 COX-2 was dissociated from the NE. On day 1 the majority of COX-2^+ M∅ had phagocytosed HK-BCG. In contrast, there was no intracellular HK-BCG detected in days 7 and 14 COX-2^+ M∅ where COX-2 was associated with the NE. However, when M∅ phagocytosed HK-BCG *in vitro*, all COX-2 was associated with the NE. Thus, the administration of HK-BCG induces the biphasic COX-2 expression in splenic M∅ of either a NE-dissociated catalytically inactive or a NE-associated catalytically active form. The catalytically inactive COX-2^+ M∅ develop microbicidal activities effectively since they lack PGE_2 biosynthesis.

Keyword: cyclooxygenase, prostaglandin E_2, macrophage

INTRODUCTION

Cyclooxygenase-2 (COX-2, prostaglandin G/H synthase-2) is induced in local macrophages (M∅) in response to exogenous and endogenous inflammatory agents and is rate-limiting for M∅ prostaglandin E_2 (PGE_2) biosynthesis. PGE_2 released by M∅ regulates various immune responses in autocrine and paracrine fashions. For example, PGE_2 inhibits IL-12 production by M∅ (36), inducible nitric oxide synthase (iNOS)/nitric oxide (NO) production (12), and NADPH oxidase with release of superoxide anion (14). In contrast, PGE_2 promotes IL-10 production by M∅ and Th2 cells (29, 32), dendritic cell antigen presentation (37), regulatory T cell differentiation and function (1), and CXCR4/stromal cell-derived factor-1 (SDF-1)-mediated hematopoietic stem cell migration (11). Regulation of these events, therefore, may depend on the regulation of PGE_2 release by COX-2^+ M∅ (6). The effective *in vivo* expression of these responses, furthermore, may depend on the presence of an adequate number of COX-2^+ M∅ in specific locations (25, 29, 31). Although the regulation of PGE_2 biosynthesis by local tissue M∅ *in vivo* has been reported, the regulatory mechanisms remain unclear and controversial (8, 13, 25, 35).

In the spleen, PGE_2-releasing M∅ (PGE_2-M∅) may interact closely with lymphocytes to induce a Th1-to-Th2 shift of immune responses (29) in chronic inflammatory diseases, which include mycobacterial infections (22), *Leishmania* infection (3), syphilitic infection (9), human immunodeficiency virus (HIV) infection progressing to acquired immunodeficiency syndrome (AIDS) (23), and animal models of autoimmune diseases that are established with Freund's complete adjuvant (heat-killed [HK] *Mycobacterium tuberculosis* in mineral oil) (2). Recently, we have found (28, 29) that various strains of mice (Balb/c, C57BL/6, IL-$10^{-/-}$) develop splenic COX-2^+ F4/80^+ M∅ not only 5 – 21 days but also 1 day (occasionally 2 – 3 more days) after intraperitoneal administration of HK-*M. bovis* Bacillus Calmette-Guérin (HK-BCG). At 5-21 days following treatment, splenic M∅ release 7 – 10-fold more PGE_2 than do those of untreated mice. In sharp contrast, COX-2 expressed by day 1 M∅ is catalytically inactive and there is no increase in PGE_2 (28). However, we found that M∅ freshly isolated from normal spleens and peritonea and treated with HK-BCG *in vitro* express catalytically active COX-2 within 1 day. Thus, on day 1 splenic M∅ treated with HK-BCG *in vivo* but not *in vitro*, appear to uniquely express catalytically inactive COX-2.

Catalytically active COX-2 is an integral membrane protein that lacks a transmembrane domain and associates with only one face of the membrane bilayer through a monotopic membrane binding domain (34). The active enzyme is localized in the nuclear envelope (NE) and the endoplasmic reticulum (ER) (17, 20, 34). PGE_2 is effectively synthesized from arachidonic acid (AA) by the combined actions of cytosolic phospholipase A_2 ($cPLA_2$), COX-2 and microsomal PGE synthase (mPGES), which are localized in the perinuclear membrane (18, 19). In this study, we have determined that COX-2 activity in splenic M∅ isolated from HK-BCG-treated mice is associated with specific subcellular localization.

MATERIALS AND METHODS

Animals. Non-pregnant female C57BL/6 mice, 8-14 weeks old, were obtained from Harlan Laboratory (Indianapolis, IN). Mice were maintained in barrier-filtered cages and fed Purina laboratory chow and tap water *ad libitum.* Experimental protocols employed in this study were approved by the Institutional Animal Care and Use Committee of Florida Atlantic University.

Treatment of mice with intraperitoneal administration of HK-BCG. As described previously (28), the cultured bacteria of *M. bovis* BCG Tokyo 172 strain were washed, autoclaved, and lyophilized. This HK-BCG powder was suspended in pyrogen-free saline and dispersed by brief (10 s) sonication immediately before use. These HK-BCG preparations contained undetectable levels of endotoxin (<0.03 EU/ml), as determined by the *Limulus* amebocyte lysate assay (Sigma Aldrich, St. Louis, MO) (28). Groups of mice (3/group) received 1 mg HK-BCG (5×10^8 bacilli/mg) intraperitoneally (i.p.) on day 0. Control mice received 0.1 ml saline. Spleens were harvested on days 0, 1, 7, and 14.

Splenic M∅ preparation. Mice were anesthetized by intraperitoneal injection of 50 mg/kg ketamine and 5 mg/kg xylazine. Spleens from each group of mice were isolated and minced with scissors. Spleen cells were suspended in RPMI 1640 plus 10% FBS at 37°C for 1 h followed by filtration through a 100-µm mesh. To enrich the M∅ fraction (24, 31), spleen cell suspensions were plated at 2×10^7 cells per 100 mm culture dish (Falcon, Oxnard, CA) and incubated at 37°C in 5% CO_2 in air. After 2 h incubation, cells were washed with Ca^{2+}-and Mg^{2+}-free phosphate-buffered saline (PBS) for removal of non-adherent cells. Culture dishes were placed on ice for 30 min before harvesting the adherent cells by scraping with a cell scraper (Corning, Corning, NY) and washing twice with serum-free RPMI 1640. Viability determined by trypan blue exclusion was >90%. Adherent spleen cells were approximately 70% M∅, estimated by phagocytosis of IgG-opsonized sheep red cells and/or cytometrically following staining with anti-F4/80 (24, 26, 31).

Treatment of splenic M∅ with HK-BCG or LPS *in vitro*. Adherent splenic M∅ obtained from normal mice as described above were plated at 10^6 cells per well of 12-well culture plates (Falcon) and incubated at 37°C in 5% CO_2 in air. Cells were cultured with 100 μg/ml HK-BCG or 1 μg/ml LPS for an additional 24 h.

Subcellular localization of COX-2 by confocal microscopy analysis. Splenic and peritoneal M∅ prepared as described above were fixed in 4% paraformaldehyde in PBS for 30 min. The fixed cells were permeabilized with PBS containing 0.1% Triton X-100 for 5 min and incubated for 3 h in blocking buffer consisting of PBS with 10% FBS at room temperature. Subsequent antibody incubations were also performed in the blocking buffer. Cells were incubated with anti-COX-2 antibody (1:500; Cayman Chemical, Ann Arbor, MI) overnight at 4°C. Subsequently, cells were washed with PBS three times and incubated with fluorescein isothiocyanate (FITC)-conjugated donkey anti-rabbit IgG (1:500; Jackson ImmunoReseach, West Glove, PA) for 1 h at room temperature. For detection of the nucleus and HK-BCG, propidium iodine (PI) was mixed at 10 μg/ml with the second antibody solution. After washing three times, cells were examined with a laser scanning confocal microscope (Bio-Rad Radiance 2100). The images were processed with Adobe Photoshop software. To confirm the immunologic specificity of the COX-2 antibody a blocking peptide (250 μg/ml) of C-terminal amino acids 570-598 of COX-2 (DPQPTKTATINASASHSRLDDINPTVLIK) (Cayman Chemical) was included in some experiments.

Subcellular fractionation. The method for subcellular fractionation was modified from that published previously (34). Splenic M∅ prepared above were resuspended in 0.1 M Tris-HCl (pH 7.5), disrupted with a Dounce homogenizer and forced through 26-gauge needles on ice. Removal of cell membranes was verified by microscopic examination. Cell debris was removed by low speed centrifugation (700 × *g* for 10 min), and the supernatants were further centrifuged at 10,000 × *g* for 10 min to collect nuclei. The resulting supernatants were subjected to ultracentrifugation at 100,000 × *g* for 90 min to prepare membrane and cytosolic fractions. Nuclei and membrane fractions were resuspended in 0.1 M Tris-HCl (pH 7.5). Protein concentrations were measured with a bicinchoninic acid assay (Pierce, Rockford, IL) and bovine serum albumin as standard.

Western blot analysis. Equal amounts of protein were loaded onto SDS-polyacrylamide minigels and separated by electrophoresis (200 V for 45 min). Proteins were then transferred to polyvinylidene difluoride (PVDF) membrane (Millipore, Bedford, MA). The membrane was blocked with 10% nonfat dry milk, and incubated with anti-COX-2 antibodies (Cayman Chemical) in 5% nonfat dry milk, overnight at 4°C. Following incubation with peroxidase-conjugated donkey anti-rabbit IgG (1:20,000; Jackson ImmunoResearch), proteins were detected by chemiluminescence (ECL plus, Amersham, Piscataway, NJ) following the manufacturer's instructions. Specificity of the COX-2 antibody was confirmed with the COX-2 blocking peptide as described above.

COX activity assay. COX activity in isolated cellular fractions was measured with a COX Assay kit (Cayman Chemical) following the manufacturer's instructions with AA as a substrate and *N,N,N',N'*-tetramethyl-*p*-phenylenediamine (TMPD) as a co-substrate. Equal amounts of protein (20 μg) were incubated at 25°C in a reaction mixture consisting of AA, TMPD and heme in 0.1 M Tris-HCl (pH 7.5). The absorbance change, due to oxidation of TMPD during the initial 5 min, was measured at 590 nm.

Mouse anti-BCG antisera. Mice were immunized intraperitoneally with 1 mg HK-BCG. Sera were isolated 14 days after HK-BCG treatment. For the detection of intracellular HK-BCG by confocal analysis, anti-BCG serum was diluted at 1:100 with blocking buffer consisting of PBS with 10% FBS. The primary antibody was detected by FITC-conjugated donkey anti-mouse IgG (Jackson ImmunoResearch).

Statistics. Differences between mean values for Fig. 3B were analyzed by Student's *t* test with the Statcel software. $P < 0.05$ is considered statistically significant.

RESULTS AND DISCUSSION

Background. Previously we demonstrated the biphasic COX-2 protein expression by splenic F4/80$^+$ M∅ after HK-BCG administration and the discordance between COX-2 expression and PGE_2 production on day 1 following treatment (28). Treatment of mice with 1 mg HK-BCG was chosen to achieve an inflammatory response comparable to that associated with mycobacterial infections, or Freund's complete adjuvant as used in models of autoimmune disease. Previous studies (30) showed that splenic M∅ isolated from untreated mice release minimal levels of PGE_2. Splenic M∅ obtained 7 or 14 days after treatment of mice with 1 mg HK-BCG and stimulated *in vitro* with either calcium ionophore A23187 or AA (a COX substrate) released more than 8 times more PGE_2 than did untreated controls (28). We have shown that PGE_2 biosynthesis by day 14 splenic M∅ is inhibited by NS-398, nimesulide or indomethacin, indicating dependence on COX-2 (29). In contrast, on days 1 and 3 following HK-BCG treatment splenic M∅ showed little increase in PGE_2 release (28).

COX and PGES are key enzymes for PGE_2 biosynthesis. We therefore investigated expression of these enzymes in splenic M∅ by Western blot analysis (28). Splenic M∅ isolated from untreated mice expressed COX-1, cytosolic PGES (cPGES) and mPGES but not COX-2. Following treatment with 1 mg HK-BCG, COX-2 was detected on days 1, 7 and 14 but not on day 3. The levels of COX-1, mPGES-1 and cPGES on days 1, 7 and 14 were similar to those in untreated splenic M∅. However, on day 1 after HK-BCG treatment, the increased COX-2 expression did not result in enhanced PGE_2 biosynthesis. Cell-free PGE_2 biosynthesis assays confirmed that COX and PGES on day 1 were catalytically inactive and active, respectively (28).

Thus, catalytically inactive and active COX-2 were associated with the PGE_2 synthesis activities of M∅ on days 1 and 7 (or 14), respectively.

Different localization of COX-2 expressed by splenic M∅ on days 1, 7 and 14 after HK-BCG treatment. To further understand the changes in COX-2 expression and activity, the subcellular localization of COX-2 in splenic M∅ has been examined by confocal microscopy. Staining of HK-BCG with PI and anti-BCG sera is shown in Fig. 1A. As shown in Fig. 1B, COX-2 in day 1 M∅ was dissociated from the PI-stained NE. PI-stained HK-BCG microbes were also detected in the day 1 M∅ (Fig. 1B). In contrast, significant numbers of M∅ on days 7 and 14 showed COX-2 localized in the NE and more diffusely distributed in the cytoplasm (Fig. 1B). The COX-2 localization in these M∅ is similar to that of catalytically active COX-2 expressed by serum-stimulated NIH/3T3 cells (17). Interestingly, however, not all MØ COX-2 was NE-associated on days 7 and 14 with some cells appearing as on day 1 with NE-dissociated COX-2. Table 1 summarizes M∅ cell counts based on NE -associated and -dissociated COX-2 distributions. On day 1, almost all COX-2^+ splenic M∅ (99.8%) expressed NE-dissociated COX-2, whereas on days 7 and 14, only 54 and 53%, respectively, of COX-2^+ M∅ had NE-dissociated COX-2 (Table 1). Significant numbers of M∅ expressing NE-dissociated COX-2 also contained intracellular PI-stained HK-BCG microbes (Fig. 1B and Table 1). We also found that M∅ expressing NE-associated COX-2 had no detectable intracellular BCG, suggesting phagocytosis-dependent NE-dissociated COX-2 expression.

***In vitro* treatment of M∅ with HK-BCG resulted in NE-associated COX-2.** To determine whether HK-BCG induces NE-dissociated COX-2 expression *in vitro*, splenic M∅ and peritoneal M∅ were isolated from normal mice, and treated *in vitro* with 100 μg/ml HK-BCG or 1 μg/ml LPS as a positive control for 24 h. Only NE-associated COX-2 expression was detected in HK-BCG- or LPS- treated splenic M∅ (Fig. 2) and peritoneal M∅ (data not shown). These COX-2^+ M∅ released significant amounts of PGE_2 when elicited with A23187 for 2 h (data not shown). Intracellular HK-BCG was also detected by PI staining (Fig. 2). Our results indicate that NE-dissociated COX-2 expression is induced by HK-BCG *in vivo* (Fig. 1B) but not *in vitro* in splenic M∅. In fact, peritoneal M∅ isolated day 1 after intraperitoneal administration of HK-BCG also expressed NE-dissociated/ catalytically inactive COX-2 but not NE-associated/catalytically active COX-2 (manuscript in preparation). Thus, our results clearly indicate that the phagocytosis of HK-BCG by M∅ *in vivo* is related to the expression of NE-dissociated COX-2 in splenic M∅ and probably also peritoneal M∅.

Differential expression of COX-2 in subcellular fractions. To further confirm that COX-2 dissociated from the NE is catalytically inactive, on days 1 and 7 splenic M∅ were homogenized and subjected to differential centrifugation. On day 7, relatively more COX-2 protein was detected in the nuclear fraction than in the membrane fraction (Fig. 3A). The profile of COX-2 distribution is similar to that determined for murine M∅ stimulated with LPS (21). Significantly, more COX activity was detected in the nuclear fraction compared to the membrane and cytosolic fractions (Fig. 3B). In contrast, on day 1 COX-2 was predominantly detected in the membrane fraction but not in the nuclear fraction. However, on day 1, there was only minimal COX activity in any of the subcellular fractions. Taken together, these results suggest that on day 1 after HK-BCG treatment COX-2 that is dissociated from the NE and localized in the membrane fraction is catalytically inactive.

Ontogenic heterogeneity between day 1 and days 7/14 splenic M∅. The differential COX-2 activities of splenic M∅ obtained on day 1 and days 7/14 (28) appear to be related to ontogenic heterogeneity of these M∅. Although both day 1 and days 7/14 COX-2$^+$ M∅ expressed F4/80 (28, 29), day 1 M∅, which seem to be resident in the spleen, directly phagocytose HK-BCG. On days 2 – 3 after *in vivo* HK-BCG treatment, COX-2 expression in splenic MØ is significantly reduced by an undetermined mechanism. Our previous studies demonstrated that days 7 and 14 PGE_2-M∅ are derived from radiosensitive bone marrow (24, 28, 31). It is likely that, at the early stages (at 1 – -2 days) after HK-BCG treatment, COX-2$^-$ M∅ precursors are induced to migrate from the bone marrow and localize in the spleen where mature forms of PGE_2-M∅ are established within 5 – 21 days (24, 31). Our results indicate that these bone marrow-derived M∅ express catalytically active COX-2 (PGE_2-MØ), apparently without the phagocytosis of HK-BCG. We have not determined whether M∅ expressing NE-dissociated COX-2 on days 7 and 14 include both resident M∅ and the recently bone marrow-derived M∅.

Cytoplasmic COX-2 in day 1 splenic M∅. Phagocytosis of HK-BCG *in vivo,* but not *in vitro,* appears to be essential for development of NE-dissociated, catalytically inactive COX-2 (Figs. 1B and 2, Table 1). Spencer *et al*. (34) reported in their analysis of COX mutants that the proteins, which lacked enzyme activity, were distributed in the microsomal membrane fraction. They suggested that these mutant proteins were mostly present as unfolded aggregates that precipitated with membrane fractions. Although they also suggested that the membrane binding domains of COX are important in maintaining the catalytic activity, a precise explanation for the association of cellular localization with enzyme activity or inactivity is unknown. Recently, D'Avila *et al.* (5) reported that intrapleural administration of live BCG induces lipid-laden pleural M∅ in a TLR2-dependent but phagocytosis-independent manner. Following either *in vivo* or *in vitro* treatment with live BCG, M∅ expressed COX-2 localized at the lipid bodies within 24 h and mediated a large amount of PGE_2 synthesis (5). In our study, lipid bodies were not specifically identified. However, we did find that COX-2 was not preferentially co-localized with intracellular HK-BCG (Fig. 1B) or lysosome-associated membrane protein 1 $(LAMP-1)^+$ late-phagosomes (data not shown). Liou *et al*. found that COX-2 was present in cytosolic vesicle-like structures in PMA-stimulated bovine aortic endothelial cells *in vitro*, and that PGI_2 synthesis by these cells was not enhanced compared to unstimulated cells (16). In PMA- and IL-1β- treated fibroblasts, catalytically active COX-2 was found in the plasma membrane co-localized with caveolin (15). Thus, regulation of COX-2 activity associated with its subcellular localization appears to be complex, dependent on cell types and specific activating agents.

Additionally, the adequate coupling of COX-2 with either PLA_2s providing substrate or the terminal PGES is important for PGE_2 synthesis (18, 19, 33). In HK-BCG treated animals, we found previously that PGES activity is intact in day 1 M∅ (28). Therefore, on day 1 mPGES and COX-2 may be in different subcellular compartments. In support of this conclusion, we have detected mPGES localized in the NE on both days 1 and 14 (data not shown).

Immunological roles of catalytically inactive $COX\text{-}2^+$ M∅. Mycobacteria including *M. bovis* BCG are powerful Th1 adjuvants and are used to induce autoimmune diseases in animal models. M∅ in response to these components become bactericidal with increases in NADPH oxidase/superoxide anion release (10), iNOS/NO production (4), and IFN-γ/IL-12/TNFα synthesis (27). These components concomitantly induce COX-2 expression and PGE_2 biosynthesis. PGE_2 down-regulates Th1 responses and microbicidal activities (7, 12, 29). It is therefore reasonable to speculate that catalytically inactive COX-2$^+$ M∅ enhance Th1 responses and development of bactericidal activities more effectively than M∅ with catalytically active COX-2.

It has been well established that bacterial immunomodulators (HK-BCG or HK-*Corynebacterium parvum* [*Propionibacterium acnes*]) given intraperitoneally attenuate the release of PGE_2 and other eicosanoids by peritoneal M∅ compared to those from untreated animals (8, 13, 25). Our present and previous findings (28) indicate that the differential subcellular localization of COX-2 in splenic M∅ following intraperitoneal administration of HK-BCG results in differing capacities for PGE_2 biosynthesis. This is the first report demonstrating that NE-dissociated COX-2, which lacks catalytic activity, is induced in local M∅ phagocytosing HK-BCG. Interestingly, NE-dissociated COX-2 expression is not seen in M∅ phagocytosing HK-BCG *in vitro*. The reason for this difference is not clear at this time. Thus, our study indicates that the generally accepted concept that in the presence of bacterial components resident COX-2-negative M∅ are converted to COX-2-positive M∅ with release of relatively large amounts of PGE_2 may need further investigation particularly with respect to the effects of *in vivo* phagocytosis of intracellular bacteria by M∅.

ACKNOWLEDGMENTS

This work was supported by NIH RO1 HL71711, DOD DAMD 17-03-1-0004, the Charles E. Schmidt Biomedical Foundation (YS) and Florida Atlantic University.

REFERENCES

1. **Baratelli F, Lin Y, Zhu L, Yang SC, Heuze-Vourc'h N, Zeng G, Reckamp K, Dohadwala M, Sharma S, and Dubinett SM.** Prostaglandin E_2 induces *FOXP3* gene expression and T regulatory cell function in human $CD4^+$ T cells. *J Immunol* 175: 1483-1490, 2005.

2. **Billiau A and Matthys P.** Modes of action of Freund's adjuvants in experimental models of autoimmune diseases. *J Leukoc Biol* 70: 849-860, 2001.

3. **Bretscher PA, Wei G, Menon JN, and Bielefeldt-Ohmann H.** Establishment of stable, cell-mediated immunity that makes "susceptible" mice resistant to Leishmania major. *Science* 257: 539-542, 1992.

4. **Chan ED, Morris KR, Belisle JT, Hill P, Remigio LK, Brennan PJ, and Riches DW.** Induction of inducible nitric oxide synthase-NO* by lipoarabinomannan of *Mycobacterium tuberculosis* is mediated by MEK1-ERK, MKK7-JNK, and NF-kappaB signaling pathways. *Infect Immun* 69: 2001-2010, 2001.

5. **D'Avila H, Melo RC, Parreira GG, Werneck-Barroso E, Castro-Faria-Neto HC, and Bozza PT.** *Mycobacterium bovis* bacillus Calmette-Guerin induces TLR2-mediated formation of lipid bodies: intracellular domains for eicosanoid synthesis in vivo. *J Immunol* 176: 3087-3097, 2006.

6. **Dubois RN, Abramson SB, Crofford L, Gupta RA, Simon LS, Van De Putte LB, and Lipsky PE.** Cyclooxygenase in biology and disease. *Faseb J* 12: 1063-1073, 1998.

7. **Edwards CK, 3rd, Hedegaard HB, Zlotnik A, Gangadharam PR, Johnston RB, Jr., and Pabst MJ.** Chronic infection due to *Mycobacterium intracellulare* in mice: association with

macrophage release of prostaglandin E_2 and reversal by injection of indomethacin, muramyl dipeptide, or interferon-gamma. *J Immunol* 136: 1820-1827, 1986.

8. **Fels AO, Pawlowski NA, Abraham EL, and Cohn ZA.** Compartmentalized regulation of macrophage arachidonic acid metabolism. *J Exp Med* 163: 752-757, 1986.

9. **Fitzgerald TJ.** The Th1/Th2-like switch in syphilitic infection: is it detrimental? *Infect Immun* 60: 3475-3479, 1992.

10. **Gangadharam PR and Edwards CK, 3rd.** Release of superoxide anion from resident and activated mouse peritoneal macrophages infected with *Mycobacterium intracellulare. Am Rev Respir Dis* 130: 834-838, 1984.

11. **Goichberg P, Kalinkovich A, Borodovsky N, Tesio M, Petit I, Nagler A, Hardan I, and Lapidot T.** cAMP-induced PKCzeta activation increases functional CXCR4 expression on human $CD34^+$ hematopoietic progenitors. *Blood* 107: 870-879, 2006.

12. **Harbrecht BG, Kim YM, Wirant EA, Simmons RL, and Billiar TR.** Timing of prostaglandin exposure is critical for the inhibition of LPS- or IFN-gamma-induced macrophage NO synthesis by PGE_2. *J Leukoc Biol* 61: 712-720, 1997.

13. **Humes JL, Burger S, Galavage M, Kuehl FA, Jr., Wightman PD, Dahlgren ME, Davies P, and Bonney RJ.** The diminished production of arachidonic acid oxygenation products by elicited mouse peritoneal macrophages: possible mechanisms. *J Immunol* 124: 2110-2116, 1980.

14. **Johnson WJ and Sung CP.** Rat macrophage treatment with lipopolysaccharide leads to a reduction in respiratory burst product secretion and a decrease in NADPH oxidase affinity. *Cell Immunol* 108: 109-119, 1987.

15. **Liou JY, Deng WG, Gilroy DW, Shyue SK, and Wu KK.** Colocalization and interaction of cyclooxygenase-2 with caveolin-1 in human fibroblasts. *J Biol Chem* 276: 34975-34982, 2001.

16. **Liou JY, Shyue SK, Tsai MJ, Chung CL, Chu KY, and Wu KK.** Colocalization of prostacyclin synthase with prostaglandin H synthase-1 (PGHS-1) but not phorbol ester-induced PGHS-2 in cultured endothelial cells. *J Biol Chem* 275: 15314-15320, 2000.

17. **Morita I, Schindler M, Regier MK, Otto JC, Hori T, DeWitt DL, and Smith WL.** Different intracellular locations for prostaglandin endoperoxide H synthase-1 and -2. *J Biol Chem* 270: 10902-10908, 1995.

18. **Murakami M, Das S, Kim YJ, Cho W, and Kudo I.** Perinuclear localization of cytosolic phospholipase A_2alpha is important but not obligatory for coupling with cyclooxygenases. *FEBS Lett* 546: 251-256, 2003.

19. **Murakami M, Naraba H, Tanioka T, Semmyo N, Nakatani Y, Kojima F, Ikeda T, Fueki M, Ueno A, Oh S, and Kudo I.** Regulation of prostaglandin E_2 biosynthesis by inducible membrane-associated prostaglandin E_2 synthase that acts in concert with cyclooxygenase-2. *J Biol Chem* 275: 32783-32792, 2000.

20. **Otto JC and Smith WL.** The orientation of prostaglandin endoperoxide synthases-1 and -2 in the endoplasmic reticulum. *J Biol Chem* 269: 19868-19875, 1994.

21. **Patel R, Attur MG, Dave M, Abramson SB, and Amin AR.** Regulation of cytosolic COX-2 and prostaglandin E_2 production by nitric oxide in activated murine macrophages. *J Immunol* 162: 4191-4197, 1999.

22. **Power CA, Wei G, and Bretscher PA.** Mycobacterial dose defines the Th1/Th2 nature of the immune response independently of whether immunization is administered by the intravenous, subcutaneous, or intradermal route. *Infect Immun* 66: 5743-5750, 1998.

23. **Salk J, Bretscher PA, Salk PL, Clerici M, and Shearer GM.** A strategy for prophylactic vaccination against HIV. *Science* 260: 1270-1272, 1993.

24. **Shibata Y.** Restoration of prostaglandin E_2-producing splenic macrophages in ^{89}Sr-treated mice with bone marrow from *Corynebacterium parvum* primed donors. *Reg Immunol* 2: 169-175, 1989.

25. **Shibata Y, Bautista AP, Pennington SN, Humes JL, and Volkman A.** Eicosanoid production by peritoneal and splenic macrophages in mice depleted of bone marrow by ^{89}Sr. *Am J Pathol* 127: 75-82, 1987.

26. **Shibata Y, Bjorkman DR, Schmidt M, Oghiso Y, and Volkman A.** Macrophage colony-stimulating factor-induced bone marrow macrophages do not synthesize or release prostaglandin E_2. *Blood* 83: 3316-3323, 1994.

27. **Shibata Y, Foster LA, Kurimoto M, Okamura H, Nakamura RM, Kawajiri K, Justice JP, Van Scott MR, Myrvik QN, and Metzger WJ.** Immunoregulatory roles of IL-10 in innate immunity: IL-10 inhibits macrophage production of IFN-gamma-inducing factors but enhances NK cell production of IFN-gamma. *J Immunol* 161: 4283-4288, 1998.

28. **Shibata Y, Gabbard J, Yamashita M, Tsuji S, Smith M, Nishiyama A, Henriksen RA, and Myrvik QN.** Heat-killed BCG induces biphasic cyclooxygenase 2^+ splenic macrophage formation--role of IL-10 and bone marrow precursors. *J Leukoc Biol* 80: 590-598, 2006.

29. **Shibata Y, Henriksen RA, Honda I, Nakamura RM, and Myrvik QN.** Splenic PGE_2-releasing macrophages regulate Th1 and Th2 immune responses in mice treated with heat-killed BCG. *J Leukoc Biol* 78: 1281-1290, 2005.

30. **Shibata Y, Nishiyama A, Ohata H, Gabbard J, Myrvik QN, and Henriksen RA.** Differential effects of IL-10 on prostaglandin H synthase-2 expression and prostaglandin E_2 biosynthesis between spleen and bone marrow macrophages. *J Leukoc Biol* 77: 544-551, 2005.

31. **Shibata Y and Volkman A.** The effect of bone marrow depletion on prostaglandin E-producing suppressor macrophages in mouse spleen. *J Immunol* 135: 3897-3904, 1985.

32. **Shinomiya S, Naraba H, Ueno A, Utsunomiya I, Maruyama T, Ohuchida S, Ushikubi F, Yuki K, Narumiya S, Sugimoto Y, Ichikawa A, and Oh-ishi S.** Regulation of TNFalpha and interleukin-10 production by prostaglandins $I_2$and E_2: studies with prostaglandin receptor-deficient mice and prostaglandin E-receptor subtype-selective synthetic agonists. *Biochem Pharmacol* 61: 1153-1160, 2001.

33. **Smith WL, DeWitt DL, and Garavito RM.** Cyclooxygenases: structural, cellular, and molecular biology. *Annu Rev Biochem* 69: 145-182, 2000.

34. **Spencer AG, Thuresson E, Otto JC, Song I, Smith T, DeWitt DL, Garavito RM, and Smith WL.** The membrane binding domains of prostaglandin endoperoxide H synthases 1 and 2. Peptide mapping and mutational analysis. *J Biol Chem* 274: 32936-32942, 1999.

35. **Tripp CS, Unanue ER, and Needleman P.** Monocyte migration explains the changes in macrophage arachidonate metabolism during the immune response. *Proc Natl Acad Sci U S A* 83: 9655-9659, 1986.

36. **van der Pouw Kraan TC, Boeije LC, Smeenk RJ, Wijdenes J, and Aarden LA.** Prostaglandin-E_2 is a potent inhibitor of human interleukin 12 production. *J Exp Med* 181: 775-779, 1995.

37. **Vassiliou E, Sharma V, Jing H, Sheibanie F, and Ganea D.** Prostaglandin E_2 promotes the survival of bone marrow-derived dendritic cells. *J Immunol* 173: 6955-6964, 2004.

FIGURE LEGENDS

Fig. 1. Subcellular localization of COX-2 expressed by splenic M∅ after HK-BCG treatment. A) Adherent splenic M∅ from animals treated with HK-BCG were stained with PI (red) mixed with normal mouse sera or HK-BCG-immunized mouse sera (green). HK-BCG microbes were detected by confocal microscopy. **B)** Groups of C57BL/6 female mice (3/group) received 1 mg HK-BCG i.p. on day 0. At indicated intervals, splenic M∅ were prepared. Cells were examined by confocal microscopy following immunofluorescence staining with anti-COX-2 (green) and PI (red) for the nucleus. COX-2-positive staining was completely blocked by a COX-2-specific blocking peptide (not shown).

Fig. 2. ***In vitro*** **treatment of M∅ with HK-BCG resulted in expression of NE-associated COX-2.** Normal splenic M∅ were treated with 100 μg/ml HK-BCG or 1 μg/ml LPS for 24 h. Cells were examined by confocal microscopy following immunofluorescence staining with anti-COX-2 (green) and PI (red) for the nucleus. Results shown are representative of results from three separate experiments.

Fig. 3. Distribution and activity of COX in subcellular fractions. Splenic M∅ were homogenized and separated into nuclear (N), microsomal membrane (M), and cytosolic (C) fractions by differential centrifugation as detailed in Materials and Methods. **A)** Protein (20 μg) from each fraction was used for detection of COX-2 by Western blot. Immunoreactivity of the COX-2 antibody was blocked by a COX-2-specific peptide (data not shown). **B)** The COX activity in each fraction was measured by using a COX Assay kit (Cayman Chemical) following

the manufacturer's instructions. The specific enzyme activities were calculated and indicated as nmol/min/mg. Differences between mean values were analyzed by Student's *t* test with the Statcel software. Mean ± SD, n=3. Double asterisks indicate statistically significant differences (*P* <0.01), compared to the activity in the N and C fractions on day 7 and in any of the fractions on day 1.

Table 1. ***Subcellular localization of COX-2 in splenic M∅ isolated from HK-BCG-treated mice***

	Days after 1 mg HK-BCG (i.p.)				
M∅ (%)	0 (untreated)	1	3	7	14
COX-2^{+} [a]	0.2 ± 0.02	79.3 ± 4.3	16.6 ± 13.0	57.5 ± 7.9	42.1 ± 7.6
NE-dissociated [b]	0	99.8 ± 0.2	99.5 ± 0.3	54.2 ± 8.2	53.4 ± 9.9
NE-dissociated with BCG [c]	0	80.3 ± 3.3	49.3 ± 13.5	42.9 ± 4.2	36.12 ± 2.6
NE-associated [d]	100	0.2 ± 0.2	0.5 ± 0.3	45.8 ± 8.2	46.6 ± 9.9
NE-associated with BCG [e]	0	0	0	<0.1	<0.1

Groups of C57BL/6 female mice (3/group) received 1 mg HK-BCG i.p. on day 0. Mice were sacrificed at indicated intervals. Spleens were harvested. Plastic adherent splenic M∅ were isolated. Subcellular localization of COX-2 in M∅ was determined by confocal microscopy of cells stained with anti-COX-2 antibody and PI as indicated in the Materials and Methods and shown in Fig. 1B. Percent COX-2^{+} M∅ was determined by counting 1000 M∅ in each spleen sample. Percent M∅ expressing either NE-associated or NE-dissociated COX-2 was determined by counting 500 COX-2^{+} M∅ in each spleen sample. For these cells, PI-stained intracellular BCG was also assessed. Mean ± SD, n=3.

[a] COX-2^{+}: percentage of total MØ that are COX-2^{+}.

[b] NE-dissociated: percentage of COX-2^{+} M∅ with NE-dissociated COX-2.

[c] NE-dissociated with BCG: percentage of NE-dissociated COX-2^{+} M∅ with PI-stained BCG.

[d] NE-associated: percentage of COX-2^{+} M∅ with NE-associated COX-2.

[e] NE-associated with BCG: percentage of NE-associated, COX-2^{+} M∅ with PI-stained BCG.

Figure 1

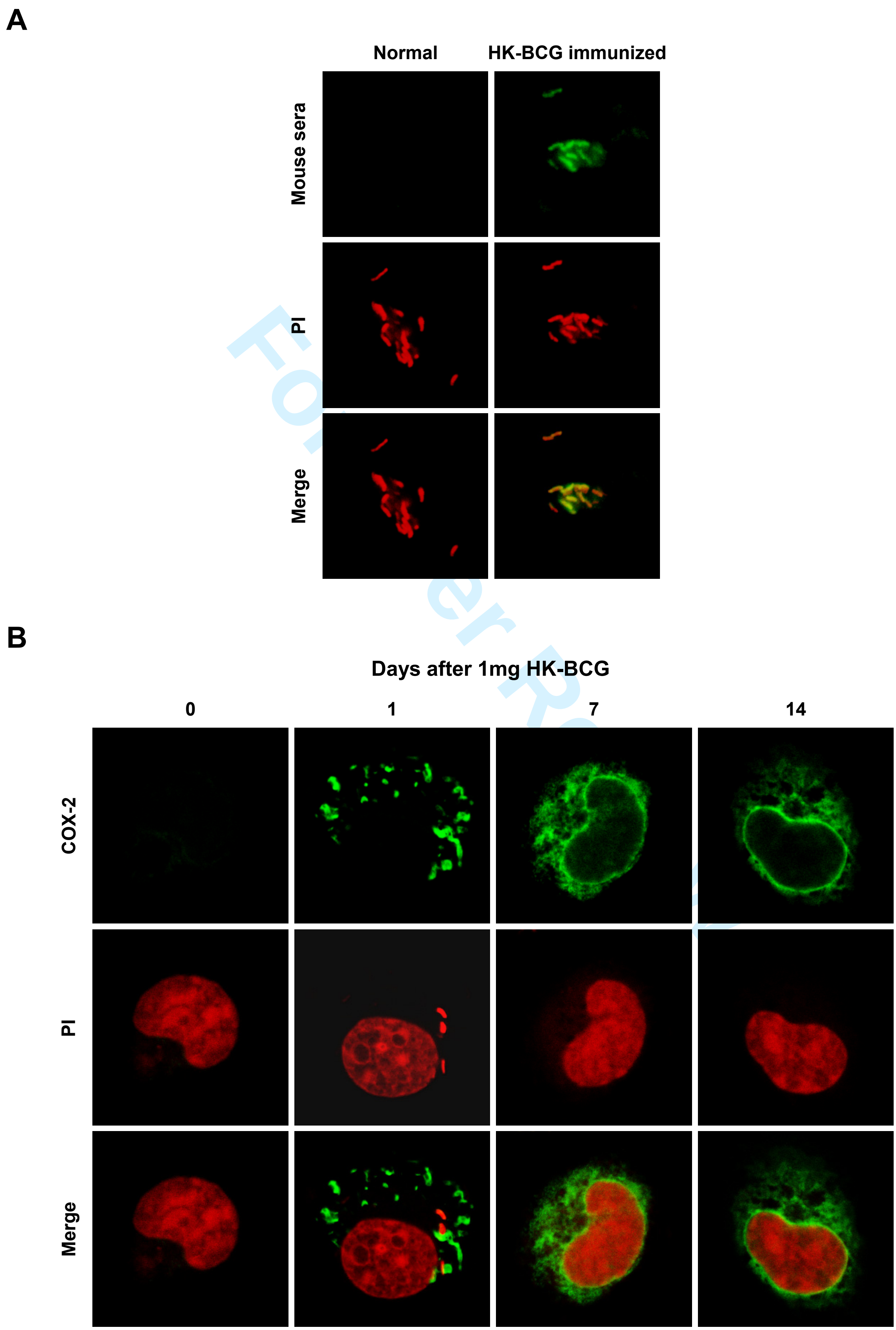
A
Normal
HK-BCG immunized
Mouse sera
PI
Merge
B
Days after 1mg HK-BCG
0
1
7
14
COX-2
PI
Merge

Figure 2

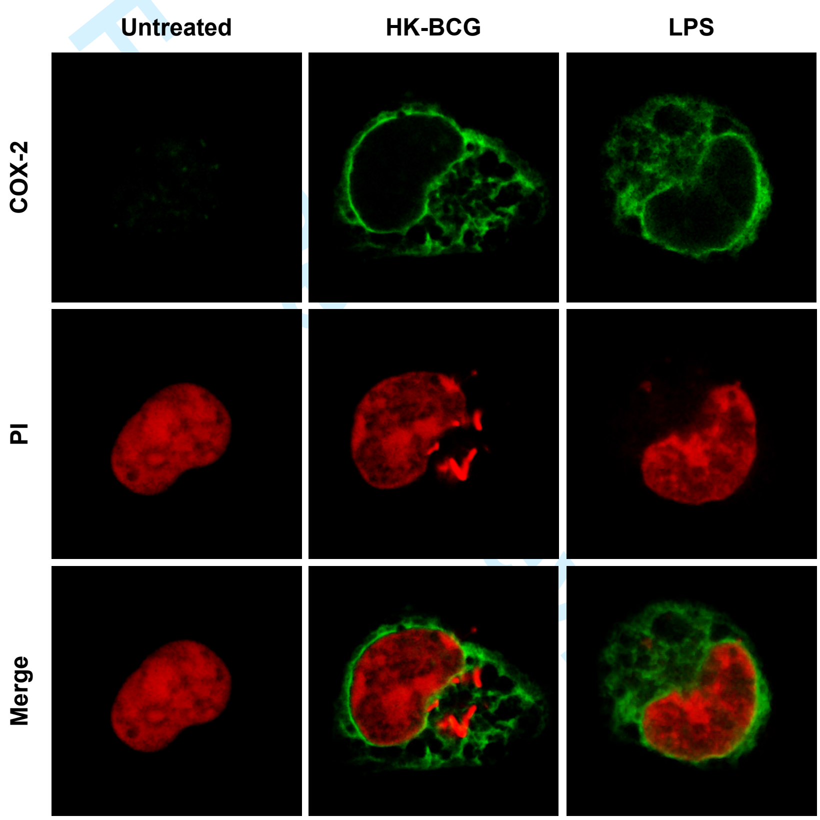

Figure 3

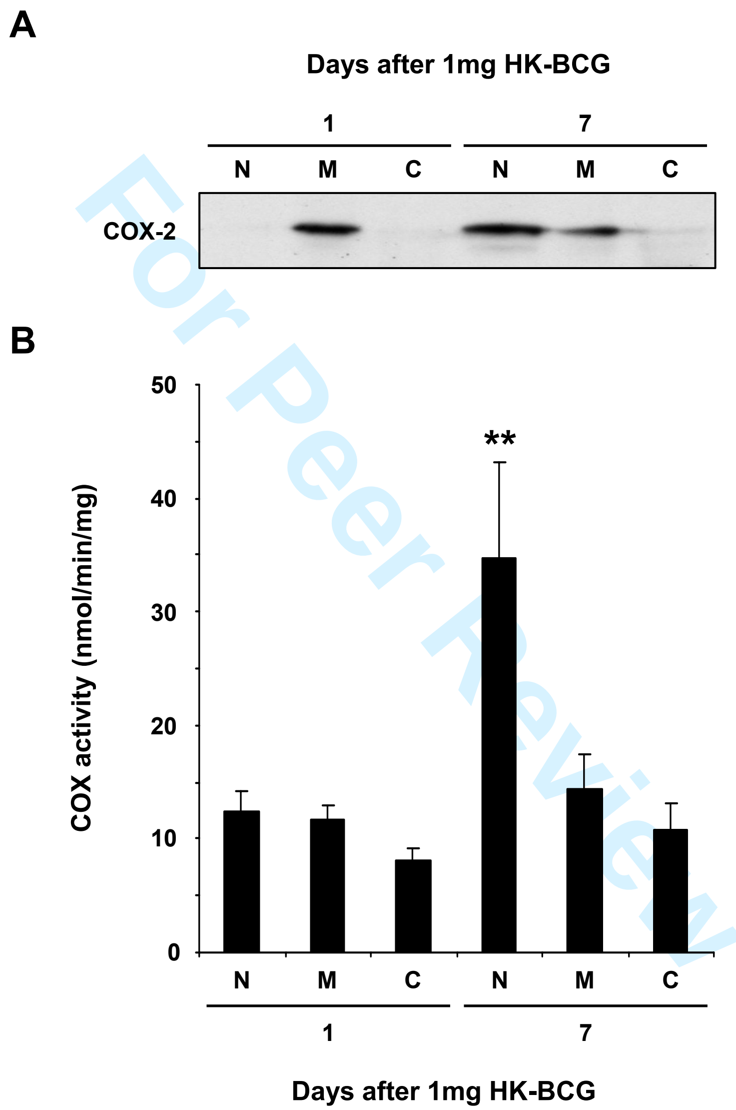
A
Days after 1mg HK-BCG
1
7
N
M
C
N
M
C
COX-2
B
COX activity (nmol/min/mg)
50
40
30
20
10
0
**
N
M
C
N
M
C
1
7
Days after 1mg HK-BCG

Glycobiochemistry accepted

Differential structure and activity between human and mouse intelectin-1: human intelectin-1 is a disulfide-linked oligomer, whereas mouse homologue is a monomer

Shoutaro Tsuji[1,2], Makiko Yamashita[2], Akihito Nishiyama[2], Tsutomu Shinohara[2], Zhongwei Li[2], Quentin N. Myrvik[3], Ruth Ann Henriksen[4], and Yoshimi Shibata[2]

[2]Biomedical Sciences, Florida Atlantic University, Boca Raton, Florida 33431; [3]404 Palmeto Dr, Caswell Beach, NC 28465; and [4]Physiology, Brody School of Medicine at East Carolina University, Greenville, NC 27834

[1]Address correspondence to: Shoutaro Tsuji, Ph.D., Biomedical Sciences, Florida Atlantic University, 777 Glades Rd, Boca Raton, Florida 33431, Phone: 561-297-0605, FAX: 561-297-2221, E-mail: stsuji@fau.edu

Short Title: Human and mouse intelectin-1

Key words: galactofuranose/galactose/innate immunity/intelectin/lectin

Abstract

Human intelectin-1 (hITLN-1) is a 120-kDa lectin recognizing galactofuranosyl residues found in cell walls of various microorganisms but not in mammalian tissues. Although mouse intelectin-1 (mITLN-1) has been identified previously, its biochemical properties and functional characteristics have not been studied. We have purified recombinant hITLN-1, and both recombinant and intestinal mITLN-1 by Ca^{2+}-dependent adsorption to galactose-Sepharose. Recombinant hITLN-1 is an oligomer, disulfide-linked through Cys-31 and Cys-48, and *N*-glycosylated at Asn-163. Despite its high homology (84.9%) with oligomeric hITLN-1, mITLN-1 isolated from C57BL/6 mice is an unglycosylated 30-kDa monomer. In competitive binding studies, hITLN-1 was eluted from galactose-Sepharose by 100 mM 2-deoxygalactose, a galactofuranosyl disaccharide, D-xylose, and both D- and L-ribose. In contrast, mITLN-1 was partially eluted by the galactofuranosyl disaccharide, and only minimally by the other saccharides indicating that the two intelectins have somewhat different lectin specificities and suggesting that mITLN-1 binds galactose-Sepharose with a higher affinity than does hITLN-1. When the N and C-terminal regions of hITLN-1 were replaced, respectively, with those of mITLN-1, galactose-Sepharose binding was associated with the C-terminal regions. Finally, hITLN-1 binding to galactose-Sepharose was not affected by substitution of the Cys residues in the N-terminal region that are necessary for oligomer formation, nor was it affected by removal of the *N*-linked oligosaccharide at Asn-163. Although both hITLN-1 and mITLN-1 recognize galactofuranosyl residues, our comparative studies, taken together, demonstrate that these intelectins have differential structures and saccharide

binding affinities.

Introduction

Human intelectin-1 (hITLN-1), a 40 or 120-kDa protein under reducing or non-reducing conditions, respectively, is a Ca^{2+}-dependent galactofuranose binding lectin, but is not a member of the C-type lectin family (Tsuji *et al*., 2001). We previously found that hITLN-1 preferentially binds galactose-Sepharose and arabinogalactan of *Nocardia rubra* (Tsuji *et al*., 2001). Galactofuranosyl residues, which are not found on mammalian tissues, stimulate specific immune responses as dominant immunogens (Daffe *et al*., 1993; Leitao *et al*., 2003; Notermans *et al*., 1988). Thus, hITLN-1 is expected to recognize not only *Nocardia rubra* (Daffe *et al*., 1993), but also *Aspergillus fumigatus* (Leitao *et al*., 2003), *Mycobacterium tuberculosis* (Pedersen and Turco, 2003), *Streptcoccus oralis* (Abeygunawardana *et al*., 1991), *Leishmania major*, and *Trypanosoma cruzi* (Suzuki *et al*., 1997), all of which contain galactofuranosyl residues in the cell walls. Some observations indicate that hITLN-1 and mouse intelectin-1 (mITLN-1) may play an immunological role against selected microorganisms or foreign antigens (Datta *et al*., 2005; Kuperman *et al*., 2005; Pemberton *et al*., 2004a, b; Wali *et al*., 2005).

The function of the host defense lectins, collectins, is dependent on oligomeric structures (Holmskov *et al*., 1995; Kurata *et al*., 1993; Super *et al*., 1992). Since intelectin (ITLN) homologues are generally oligomeric (Abe *et al*., 1999; Chamow and Hedrick, 1986; Nagata, 2005; Nishihara *et al*., 1986; Roberson and Barondes, 1982; Suzuki *et al*., 2001; Tsuji *et al*., 2001), this structure may influence their function. In the present study, we found that most mammalian ITLNs have ten conserved Cys residues but two of these are not found in the N-terminal regions of mouse and rat ITLNs (supplementary data). We hypothesized that the conserved Cys residues, Cys-31 and Cys-48 in hITLN-1, form disulfide bonds resulting in an oligomeric structure. Since mITLN-1 lacks these Cys residues, we hypothesized that the quaternary structure and carbohydrate recognition specificity of mITLN-1 differ from those of hITLN-1.

To test these hypotheses, recombinant mITLN-1 and mITLN-1 isolated from the small intestine of C57BL/6 mice were purified by adsorption to galactose-Sepharose. The properties of recombinant mITLN-1 were compared to those of recombinant hITLN-1. To determine the possible structural role of the conserved Cys residues present in hITLN-1, but not in mITLN-1, mutant forms of hITLN-1 were prepared in which the two Cys residues were replaced with Ser. In addition, the N and C terminal regions of hITLN-1 were replaced with the corresponding regions of mITLN-1. Structural features and galactose-Sepharose binding properties of the mutant and chimeric ITLNs were examined. Despite the 84.9% sequence homology between these two proteins, we have found significant structural and functional differences.

Results

Comparison of hITLN-1 and mITLN-1 structures

Conserved Cys residues often contribute to the three-dimensional structure of proteins including oligomeric structures. Thus absence or mutation of these residues can have significant effects on the structure and function of proteins. As reported previously for native hITLN-1 (Tsuji *et al*., 2001), recombinant hITLN-1 was detected as a 120-kDa protein on Western blotting under non-reducing conditions. However, recombinant mITLN-1 was a 30-kDa protein under non-reducing conditions (figure 1). Under reducing conditions, recombinant hITLN-1 and mITLN-1 appeared as 40- and 34-kDa bands, respectively. Since the predicted molecular weights of mature hITLN-1 and mITLN-1 are about 33 k, these results suggested that mITLN-1 is a monomer, in contrast to hITLN-1, which is a disulfide-linked homooligomer. To confirm that recombinant mITLN-1 is similar in structure to native mITLN-1, intestinal mITLN-1 was isolated from C57BL/6 mice as described under "Materials and Methods." Intestinal mITLN-1 showed 30- and 34-kDa bands under non-reducing and reducing conditions, respectively, identical to those of recombinant mITLN-1 (figure 1).

Location of intermolecular disulfide bonds in hITLN-1

To analyze which Cys residues form intermolecular disulfide bonds in hITLN-1, we prepared recombinant chimeric molecules from hITLN-1 and mITLN-1. Figure 2 shows the regions of hITLN-1 and mITLN-1 that were exchanged to form chimeras. Figure 3A shows that the molecular mass for a chimeric molecule consisting of the N-terminus of hITLN-1 and the C-terminus of mITLN-1 (Hu/Mo chimeric ITLN-1) was similar to that for hITLN-1 under non-reducing and reducing conditions. On the other hand, a chimeric molecule composed of the N-terminus of mITLN-1 and the C-terminus of hITLN-1 (Mo/Hu chimeric ITLN-1) had a molecular mass similar to mITLN-1 (figure 3A). These results indicate that disulfide bonds in the N-terminus link monomers of hITLN-1.

hITLN-1, but not mITLN-1, contains Cys-31 and Cys-48, the Cys residues conserved in mammalian ITLNs (supplementary data and figure 2). To determine whether these Cys residues form the intermolecular disulfide bonds linking hITLN-1 monomers, each Cys residue was replaced with Ser. As shown in figure 3A, recombinant hITLN-1 with Ser substituted for Cys-48 (48C>S hITLN-1) showed a distinct 60-kDa band and a faint 32-kDa band under non-reducing conditions. Furthermore, recombinant hITLN-1 with Ser substituted for both Cys-31 and Cys-48 (31,48C>S hITLN-1) showed only a 32-kDa band under non-reducing conditions. Under reducing condition, both mutants were detected as a 40-kDa band, the same as intact hITLN-1. Recombinant hITLN-1 with Ser substituted for Cys-31(31C>S hITLN-1) showed a distinct 32-kDa band and a faint 60-kDa band under non-reducing conditions (figure 3B). Thus, the mutation of either Cys-31 or Cys-48 prevented formation of 120-kDa oligomeric hITLN-1, although the mutants bound to galactose-Sepharose. These results suggest that both Cys-31 and Cys-48 form intermolecular disulfide bonds in hITLN-1, and that 31,48C>S hITLN-1 is produced as a monomeric form, whereas 48C>S hITLN-1 is mainly secreted as a dimeric form. Although our previous study (Tsuji *et al.*, 2001) indicated hITLN-1 was a homotrimer based on the molecular masses, 40- and 120-kDa, under reducing and non-reducing conditions, respectively, the present results suggest that hITLN-1 may be a homotetramer.

Location of glycosylation site in hITLN-1

Because the reduced mITLN-1 showed a 34-kDa band in agreement with the predicted molecular weight, it may not be glycosylated despite the presence of a glycosylation site at Asn-154. This was confirmed by treatment of mITLN-1 with peptide N-glycanase F (PNGase F) which did not alter the migration of proteins (figure 4). hITLN-1 contains potential *N*-glycosylation sites at Asn-154 and Asn-163. To determine whether Asn-163 in hITLN-1 is an *N*-glycosylation site, we prepared recombinant hITLN-1, substituting Lys, the corresponding residue from mITLN-1, for Asn-163 (163N>K hITLN-1). As shown in figure 4, 163N>K hITLN-1 migrated at 110-kDa under non-reducing conditions. After reduction, only a 34-kDa band was seen, which corresponded to the band of reduced hITLN-1 treated with PNGase F (figure 4). These results indicate that hITLN-1, but not mITLN-1, has an *N*-linked oligosaccharide present at Asn-163 and further suggest that Asn-154 is not glycosylated in either hITLN-1 or mITLN-1.

Differential saccharide binding affinities between hITLN-1 and mITLN-1

To determine the affinities of hITLN-1 and mITLN-1 for galactose, hITLN-1 or mITLN-1 was competitively eluted from galactose-Sepharose with 100 mM galactose or deoxygalactose in 10 mM Ca^{2+}. As shown in figure 5A, hITLN-1 was partially eluted by galactose and completely eluted by 2-deoxygalactose, whereas mITLN-1 was poorly eluted by either galactose. Neither hITLN-1 nor mITLN-1 was eluted by 6-deoxygalactose. These results indicate that the affinities of hITLN-1 and mITLN-1 for these galactoses differ and suggest that mITLN-1 has a higher affinity for galactose than does hITLN-1. As shown in figure 5A, hITLN-1 and mITLN-1 were, respectively, completely and partially (33%) eluted by 2-acetamido-2-deoxy-4-O-beta-D-galactofuranosyl-D-glucopyranose (GalfG). However, neither hITLN-1 nor mITLN-1 was eluted by lactose, melibiose, 2-acetamido-2-deoxy-4-O-beta-D-galactopyranosyl-D-glucopyranose (GalpG), the galactopyranoside isomer of GalfG, or N-acetylglucosamine (figure 5A). These results indicate that both hITLN-1 and mITLN-1 recognize a galactofuranosyl- but not a galactopyranosyl-containing saccharide. Additionally, hITLN-1 was eluted by D-ribose, L-ribose, and D-xylose. In contrast, mITLN-1 was poorly eluted by these pentoses (figure 5B). These results again suggest that mITLN-1 binds to an immobilized galactose more strongly than hITLN-1. To further characterize the relative binding affinities of hITLN-1 and mITLN-1 to galactose-Sepharose, the galactose concentration dependence for competitive inhibition of binding was investigated (figure 5C). The results indicate that mITLN-1 had a higher affinity for the immobilized galactose than hITLN-1.

To investigate whether the oligomeric structure of hITLN-1 affects binding affinity for galactose-Sepharose, the binding of chimeric molecules and site-specific mutants prepared above was examined by competitive elution with 100 mM galactose or 2-deoxygalactose, which showed clearly distinct elution patterns for hITLN-1 and mITLN-

1 (figure 5A). As shown in figure 6, hITLN-1 was completely and partially eluted by 2-deoxygalactose and galactose, respectively. Relatively less mITLN-1 was eluted by these monosaccharides. The oligomeric Hu/Mo chimeric ITLN-1 had an elution pattern similar to that of mITLN-1, while the elution pattern for monomeric Mo/Hu chimeric ITLN-1 was similar to that for hITLN-1. Furthermore, the elution patterns for 48C>S hITLN-1 and monomeric 31,48C>S hITLN-1 were similar to that for intact hITLN-1. These results suggest that the C-terminal regions (residues 168-313) of hITLN-1 and mITLN-1 predominate in determining the affinity for galactose-Sepharose, and that the oligomeric structure of hITLN-1 did not distinctly affect binding affinity for galactose-Sepharose.

Discussion

In mammals, highly homologous proteins frequently have similar oligomeric structures. For the mammalian lectins hITLN-1 and mITLN-1, which have a high degree of sequence homology (84.9%), our study indicates both significant differences and similarities in these structures and activities as follows: (i) hITLN-1 is a 120-kDa disulfide-linked, and *N*-glycosylated homooligomer, whereas mITLN-1 is a 30-kDa non-glycosylated monomer; (ii) the disulfide bonds linking hITLN-1 monomers appear to be formed by Cys-31 and Cys-48 residues which are not conserved in mITLN-1; (iii) hITLN-1, but not mITLN-1, has one *N*-linked oligosaccharide at Asn-163; (iv) the saccharide binding properties differ between hITLN-1 and mITLN-1 and suggest a higher affinity of mITLN-1 for galactose-Sepharose; (v) the distinctive binding is attributed to the amino acid sequences of the C-terminal regions, but not to the oligomeric structure of hITLN-1; and, (vi) finally, both hITLN-1 and mITLN-1 specifically bind galactofuranosyl residues.

Although the N-terminal regions of ITLN homologues have little amino acid sequence homology, most have two or more non-conserved Cys in this region without a predicted signal sequence (supplementary data; Abe *et al*., 1999; Chamow and Hedrick, 1986; Chang *et al*., 2004; Komiya *et al*., 1998; Lee *et al*., 1997, 2001, 2004; Nagata *et al*., 2003, 2005; Nishihara *et al*., 1986; Pemberton *et al*., 2004a; Roberson and Barondes, 1982; Schaffler *et al*., 2005; Suzuki *et al*., 2001; Tsuji *et al*., 2001). These non-conserved Cys may be related to oligomeric structures. In fact, some ITLN homologues, hITLN-1 (Suzuki *et al*., 2001; Tsuji *et al*., 2001), cortical granule lectin (Chamow and Hedrick, 1986; Nishihara *et al*., 1986; Roberson and Barondes, 1982), Xenopus embryonic epidermal lectin (XEEL) (Nagata, 2005), and ascidian galactose-specific lectin (Abe *et al*., 1999), are disulfide-linked oligomers although the location of the intermolecular disulfide bonds has not been reported previously. Rat, mouse, grass carp, and zebrafish ITLNs and *Xenopus laevis* serum lectin type 2 have no Cys in the N-terminal regions, which are followed by the predicted signal sequences (supplementary data). Thus, in rodents and fish, ITLN homologues may be monomeric.

The chimeric molecules and site-specific mutants used in this study contain the conserved Cys residues present in ITLN homologues (figure 2 and supplementary data) and retain the capacity to bind galactose-Sepharose. Thus, these molecules have the intramolecular disulfide bonds associated with the monomeric structure of ITLN. Since replacement of Cys-31 or Cys-48 in hITLN-1 with Ser produced, respectively, mainly a 32-kDa monomer or a 60-kDa homodimer (figure 3B), hITLN-1 monomer could form a Cys-31-Cys-31 disulfide-linked homodimer stably and Cys-48 could be used for polymerization of this homodimer. Since Cys-48-Cys-48 homodimer was unstable, intact hITLN-1 would form an even oligomer, a tetramer rather than a trimer. Alternatively, Cys-31-Cys-48 disulfide bonds might form between adjacent monomeric subunits.

The oligosaccharide-deficient hITLN-1 was secreted into culture media and also bound to galactose-Sepharose (figure 4). Furthermore, Mo/Hu chimeric ITLN-1, predicted to be non-glycosylated because it lacks Asn-163, had the same molecular mass as mITLN-1 (figure 3B), but a saccharide binding affinity similar to hITLN-1 (figure 6). Thus, the *N*-linked oligosaccharide of hITLN-1 is not required for protein secretion or galactose-Sepharose binding. In contrast, XEEL, an ITLN homologue in *Xenopus laevis*, requires glycosylation for secretion (Nagata, 2005). This distinction may be a consequence of the substituted amino acid: for XEEL the glycosylated Asn was replaced by Gln whereas for hITLN-1 the corresponding residue was replaced by Lys as is present in mITLN-1. Oligosaccharides of glycoproteins may also serve as ligands for binding to other lectin molecules. An oligosaccharide of cortical granule lectin, an ITLN homologue forming the fertilization envelope in *Xenopus laevis* (Gerton and Hedrick, 1986; Quill and Hedrick, 1996), is necessary for ligation to galectin-VIIa (Shoji *et al*., 2005) and the blood-group-B-active trisaccharides are related to cell-cell adhesion (Nomura *et al*., 1998). However, no specific role for the oligosaccharide in hITLN-1 has been identified.

Permberton *et al.* (2004a) reported that both Balb/c and 129/SvEv strains of mice have mITLN-1 and mITLN-2, a mITLN-1 paralog. In contrast, both C57BL/6 and C57BL/10 mice have only the mITLN-1 gene. Despite significant intestinal mITLN-1 mRNA expression in untreated and *Trichinella spiralis*-infected C57BL/10 mice, mITLN-1 protein levels were undetectable in samples isolated from these mice (Pemberton *et al*., 2004a). However, this study has clearly demonstrated that mITLN-1, detected by our ITLN-1 antibody, can be isolated from the small intestines of normal C57BL/6 mice by galactose-Sepharose affinity adsorption.

The hITLN-1 mRNA level increases in airway epithelial cells from individuals with asthma (Kuperman *et al*., 2005) or in primary mesothelial cells following SV40 infection and asbestos exposure (Wali *et al*., 2005). Others have shown that infection with *Trichinella spiralis* (Pemberton *et al*., 2004a, b) or *Trichuris muris* (Datta *et al*., 2005) induced mITLN-1 and mITLN-2 mRNA expression. These observations and the galactofuranose binding activity of hITLN-1 and mITLN-1 suggest that ITLN homologues have an immunoregulatory role in host defense. For instance, the serum ITLN homologue of ascidian (galactose-specific lectin) functions as an opsonin (Abe *et al*., 1999). On the other hand, hITLN-1 also designated a glycosylphospatidylinositol-anchored intestinal lactoferrin receptor (Suzuki *et al*., 2001), HL-1 which is expressed in vascular endothelial cells (Lee *et al*., 2001), or omentin which is found in adipose tissue (Schaffler *et al*., 2005) and human visceral fat (unpublished data). However, we have not detected mITLN-1 mRNA in cardiovascular tissues or visceral fat of C57BL/6 mice (unpublished data). Because of these differences in expression and the described differences in structure and ligand specificity, the physiological function of mITLN-1 may differ from that of hITLN-1. Recently, it was reported that swine intelectin, which is expected to be oligomeric (supplementary data), is associated with lipid rafts on the enterocyte brush border (Wrackmeyer *et al*., 2006). It is possible that mITLN-1 is similarly located. Additional investigation will be required to further establish the physiological function of ITLN-1 in both humans and mice.

Materials and methods

Purification of intestinal mITLN-1

Small intestines of mice were isolated from female 8-wk-old C57BL/6 mice (Harlan Laboratory, Indianapolis IN). The following purification procedures were carried out at 4ºC. The inside of a small intestine (approximately 0.8 g) was washed with 5 ml of saline, minced with scissors, and homogenized with a Teflon homogenizer in 10 ml of 20 mM Tris-buffered saline (pH 7.5) (TBS) containing 1% Nonidet P-40, 10 mM $CaCl_2$, and protease inhibitor cocktail (Sigma, St. Louis MO). The homogenate was incubated for 1 h and centrifuged (1,800 *g*, 10 min). The supernatants (10 ml) were mixed with 10 µl of galactose-Sepharose, prepared by incubating epoxy-activated Sepharose 6B (Amersham Pharmacia Biotech, Piscataway NJ) with galactose, and incubated for 18 h. After washing four times with TBS containing 1% Nonidet P-40 and 10 mM $CaCl_2$, mITLN-1 was eluted with 40 µl of TBS containing 10 mM ethylenediamine tetra-acetic acid (EDTA).

cDNA cloning of hITLN-1 and mITLN-1

cDNA encoding the open reading frame of mITLN-1 was cloned by reverse transcription-polymerase chain reaction (PCR). Primers were designed on the basis of a reported mITLN-1 sequence (GenBank accession no. AB016496) (5'-ATG ACC CAA CTG GGA TTC CTG-3' and 5'-TCA GCG ATA AAA CAG AAG CAC G-3') (Komiya *et al*., 1998). cDNA was synthesized from small intestinal total RNA of C57BL/6 mice using an oligo dT primer and SuperScript II Reverse Transcriptase (Invitrogen, Carlsbad CA). A single band was amplified by PCR using these primers, cDNA, and Ampli-Taq

Gold (Applied Biosystems, Foster City CA) (25 cycles, 94ºC for 30 s, 58ºC for 30 s, and 72ºC for 30 s). The PCR products were cloned and sequenced. The mITLN-1 sequence of C57BL/6 mice contained several silent mutations when compared to the reported sequence, but was the same as a sequence reported by Pemberton *et al.* (2004a) cDNA of hITLN-1 was prepared as described previously (Tsuji *et al*., 2001). Point mutations of hITLN-1 were constructed by using GeneTailor Site-Directed Mutagenesis System (Invitrogen). cDNAs for hITLN-1/mITLN-1 chimeras were made by exchange into an open reading frame at a *Kpn* I site.

Preparation of recombinant ITLN-1

RK-13 cells, a rabbit kidney cell line, were cultured in Eagle's minimum essential medium containing 5% fetal bovine serum. cDNAs of ITLN-1 were inserted into mammalian cell expression vector pEF-BOS (Mizushima and Nagata, 1990), and transfected into RK-13 cells with Lipofectamine 2000 (Invitrogen). The transfected RK-13 cells were incubated for 72 h at 37ºC. Recombinant ITLN-1 was purified from the culture supernatants of transfected cells using galactose-Sepharose as described above.

Deglycosylation

To determine whether hITLN-1 and mITLN-1 have *N*-linked oligosaccharides, the recombinant ITLN-1 preparations were digested by PNGase F (New England Biolabs, Ipswich MA) according to the manufacture’s instructions.

Cross-reactive polyclonal antibodies against hITLN-1 and mITLN-1 (anti-ITLN-1)

For preparation of anti-ITLN-1, a NZW rabbit was immunized subcutenously with 2 x 10^8 RK-13 cells transfected with mITLN-1 in complete Freund's adjuvant. After boosting twice with the same cells in incomplete Freund's adjuvant, polyclonal antibodies were isolated from serum by precipitation with 33% saturated ammonium sulfate. Anti-ITLN-1 was further purified by affinity chromatography on Affi-gel 10 (Bio-Rad) covalently bound to purified recombinant hITLN-1 and elution with 3.5 M NaSCN. The eluate was dialyzed against TBS. The cross-reactivity of anti-ITLN-1 against hITLN-1 and mITLN-1 was confirmed by Western blotting (figures 1, 3 and 4) and enzyme-linked immunosorbent assay (data not shown).

Western blotting

ITLN-1 purified by galactose-Sepharose was resolved by 10% sodium dodecyl sulfate-polyacrylamide gel electrophoresis (SDS-PAGE) under non-reducing or reducing conditions and transferred to polyvinylidene difluoride membranes (Immobilon-P, Millipore, Billerica MA). The membranes were blocked with 5% non-fat milk, and then treated for 3 h at 22ºC with 1 μg/ml anti-ITLN-1 in 5% non-fat milk. After washing, the membranes were treated with horseradish peroxidase-conjugated donkey anti-rabbit IgG (Jackson ImmunoResearch, West Glove PA) and developed with ECL plus (Amersham Pharmacia Biotech).

Competitive binding of ITLN-1 to saccharides

Galactose-Sepharose bound to recombinant hITLN-1, mITLN-1, mutated ITLN-1 or chimeric ITLN-1 was prepared as described above. The bound proteins were eluted with TBS plus 10 mM EDTA or TBS plus 10 mM $CaCl_2$ and 100 mM selected mono/disaccharides. The saccharides included 2-acetamido-2-deoxy-4-O-beta-D-galactofuranosyl-D-glucopyranose (GalfG, Toronto Research Chemicals, North York, ON, Canada) and those listed in the legend for figure 5 (obtained from Aldrich, Milwaukee WI). The relative concentration of ITLN in the eluate was assessed following resolution by reduced 10% SDS-PAGE and staining with Coomassie blue. Densities of the stained bands were measured with image analysis software (Yab GelImage; http://homepage.mac.com/yabyab/).

Acknowledgements

This study was supported by NIH RO1 HL7171, DOD DAMD 17-03-1-0004 & the Charles E. Schmidt Biomedical Foundation (YS).

Abbreviations

31C>S hITLN-1, hITLN-1 with Ser substituted for Cys-31; 31,48C>S hITLN-1, hITLN-1 with Ser substituted for both Cys-31 and Cys-48; 48C>S hITLN-1, hITLN-1 with Ser substituted for Cys-48; 163N>K hITLN-1, hITLN-1 with Lys substituted for Asn-163; EDTA, ethylenediamine tetra-acetic acid; GalfG, 2-acetamido-2-deoxy-4-O-beta-D-galactofuranosyl-D-glucopyranose; GalpG, 2-acetamido-2-deoxy-4-O-beta-D-galactopyranosyl-D-glucopyranose; hITLN-1, human intelectin-1; Hu/Mo chimeric ITLN-1, a chimeric molecule consisting of the N-terminus of hITLN-1 and the C-terminus of mITLN-1; ITLN, intelectin; mITLN-1, mouse intelectin-1; Mo/Hu chimeric ITLN-1, a chimeric molecule composed of the N-terminus of mITLN-1 and the C-terminus of hITLN-1; PCR, polymerase chain reaction; PNGase F, peptide N-glycanase F; SDS-PAGE, sodium dodecyl sulfate-polyacrylamide gel electrophoresis; TBS, 20 mM Tris-buffered saline, pH 7.5; XEEL, Xenopus embryonic epidermal lectin.

References

Abe, Y., Tokuda, M., Ishimoto, R., Azumi, K. and Yokosawa, H. (1999) A unique primary structure, cDNA cloning and function of a galactose-specific lectin from ascidian plasma. *Eur. J. Biochem.*, **261**, 33-39.

Abeygunawardana, C., Bush, C. A. and Cisar, J. O. (1991) Complete structure of the cell surface polysaccharide of *Streptococcus oralis* C104: a 600-MHz NMR study. *Biochemistry*, **30**, 8568-8577.

Chamow, S. M. and Hedrick, J. L. (1986) Subunit structure of a cortical granule lectin involved in the block to polyspermy in *Xenopus laevis* eggs. *FEBS Lett.*, **206**, 353-357.

Chang, B. Y., Peavy, T. R., Wardrip, N. J. and Hedrick, J. L. (2004) The *Xenopus laevis* cortical granule lectin: cDNA cloning, developmental expression, and identification of the eglectin family of lectins. *Comp. Biochem. Physiol. A*, **137**, 115-129.

Daffe, M., McNeil, M. and Brennan, P. J. (1993) Major structural features of the cell wall arabinogalactans of *Mycobacterium*, *Rhodococcus*, and *Nocardia* spp. *Carbohydr. Res.*, **249**, 383-398.

Datta, R., deSchoolmeester, M. L., Hedeler, C., Paton, N. W., Brass, A. M. and Else, K. J. (2005) Identification of novel genes in intestinal tissue that are regulated after infection with an intestinal nematode parasite. *Infect. Immun.*, **73**, 4025-4033.

Gerton, G. L. and Hedrick, J. L. (1986) The vitelline envelope to fertilization envelope conversion in eggs of *Xenopus laevis*. *Dev. Biol.*, **116**, 1-7.

Holmskov, U., Laursen, S. B., Malhotra, R., Wiedemann, H., Timpl, R., Stuart, G. R., Tornoe, I., Madsen, P. S., Reid, K. B. and Jensenius, J. C. (1995) Comparative study of the structural and functional properties of a bovine plasma C-type lectin, collectin-43, with other collectins. *Biochem. J.*, **305**, 889-896.

Komiya, T., Tanigawa, Y. and Hirohashi, S. (1998) Cloning of the novel gene intelectin, which is expressed in intestinal paneth cells in mice. *Biochem. Biophys. Res. Commun.*, **251**, 759-762.

Kuperman, D. A., Lewis, C. C., Woodruff, P. G., Rodriguez, M. W., Yang, Y. H., Dolganov, G. M., Fahy, J. V. and Erle, D. J. (2005) Dissecting asthma using focused transgenic modeling and functional genomics. *J. Allergy Clin. Immunol.*, **116**, 305-311.

Kurata, H., Cheng, H. M., Kozutsumi, Y., Yokota, Y. and Kawasaki, T. (1993) Role of the collagen-like domain of the human serum mannan-binding protein in the activation of complement and the secretion of this lectin. *Biochem. Biophys. Res. Commun.*, **191**, 1204-1210.

Lee, J. K., Baum, L. G., Moremen, K. and Pierce, M. (2004) The X-lectins: a new family with homology to the *Xenopus laevis* oocyte lectin XL-35. *Glycoconj. J.*, **21**, 443-450.

Lee, J. K., Buckhaults, P., Wilkes, C., Teilhet, M., King, M. L., Moremen, K. W. and Pierce, M. (1997) Cloning and expression of a *Xenopus laevis* oocyte lectin and characterization of its mRNA levels during early development. *Glycobiology*, **7**, 367-372.

Lee, J. K., Schnee, J., Pang, M., Wolfert, M., Baum, L. G., Moremen, K. W. and Pierce, M. (2001) Human homologs of the *Xenopus* oocyte cortical granule lectin XL35. *Glycobiology*, **11**, 65-73.

Leitao, E. A., Bittencourt, V. C., Haido, R. M., Valente, A. P., Peter-Katalinic, J., Letzel, M., de Souza, L. M. and Barreto-Bergter, E. (2003) Beta-galactofuranose-containing O-linked oligosaccharides present in the cell wall peptidogalactomannan of *Aspergillus fumigatus* contain immunodominant epitopes. *Glycobiology*, **13**, 681-692.

Mizushima, S. and Nagata, S. (1990) pEF-BOS, a powerful mammalian expression vector. *Nucleic Acids Res.*, **18**, 5322.

Nagata, S. (2005) Isolation, characterization, and extra-embryonic secretion of the *Xenopus laevis* embryonic epidermal lectin, XEEL. *Glycobiology*, **15**, 281-290.

Nagata, S., Nakanishi, M., Nanba, R. and Fujita, N. (2003) Developmental expression of XEEL, a novel molecule of the *Xenopus* oocyte cortical granule lectin family. *Dev. Genes Evol.*, **213**, 368-370.

Nishihara, T., Wyrick, R. E., Working, P. K., Chen, Y. H. and Hedrick, J. L. (1986) Isolation and characterization of a lectin from the cortical granules of *Xenopus laevis* eggs. *Biochemistry*, **25**, 6013-6020.

Nomura, K. H., Kobayashi, R., Hirabayashi, Y., Fujisue-Sakai, M., Mizuguchi, S. and Nomura, K. (1998) Involvement of blood-group-B-active trisaccharides in Ca^{2+}-dependent cell-cell adhesion in the *Xenopus* blastula. *Dev. Genes Evol.*, **208**, 9-18.

Notermans, S., Veeneman, G. H., van Zuylen, C. W., Hoogerhout, P. and van Boom, J. H. (1988) (1-5)-linked beta-D-galactofuranosides are immunodominant in extracellular polysaccharides of *Penicillium* and *Aspergillus* species. *Mol. Immunol.*, **25**, 975-979.

Pedersen, L. L. and Turco, S. J. (2003) Galactofuranose metabolism: a potential target for antimicrobial chemotherapy. *Cell. Mol. Life Sci.*, **60**, 259-266.

Pemberton, A. D., Knight, P. A., Gamble, J., Colledge, W. H., Lee, J. K., Pierce, M. and Miller, H. R. (2004a) Innate BALB/c enteric epithelial responses to *Trichinella spiralis*: inducible expression of a novel goblet cell lectin, intelectin-2, and its natural deletion in C57BL/10 mice. *J. Immunol.*, **173**, 1894-1901.

Pemberton, A. D., Knight, P. A., Wright, S. H. and Miller, H. R. (2004b) Proteomic analysis of mouse jejunal epithelium and its response to infection with the intestinal nematode, *Trichinella spiralis*. *Proteomics*, **4**, 1101-1108.

Quill, T. A. and Hedrick, J. L. (1996) The fertilization layer mediated block to polyspermy in *Xenopus laevis*: isolation of the cortical granule lectin ligand. *Arch. Biochem. Biophys.*, **333**, 326-332.

Roberson, M. M. and Barondes, S. H. (1982) Lectin from embryos and oocytes of *Xenopus laevis*. Purification and properties. *J. Biol. Chem.*, **257**, 7520-7524.

Schaffler, A., Neumeier, M., Herfarth, H., Furst, A., Scholmerich, J. and Buchler, C. (2005) Genomic structure of human omentin, a new adipocytokine expressed in omental adipose tissue. *Biochim. Biophys. Acta*, **1732**, 96-102.

Shoji, H., Ikenaka, K., Nakakita, S., Hayama, K., Hirabayashi, J., Arata, Y., Kasai, K., Nishi, N. and Nakamura, T. (2005) *Xenopus* galectin-VIIa binds N-glycans of members of the cortical granule lectin family (xCGL and xCGL2). *Glycobiology*, **15**, 709-720.

Super, M., Gillies, S. D., Foley, S., Sastry, K., Schweinle, J. E., Silverman, V. J. and Ezekowitz, R. A. (1992) Distinct and overlapping functions of allelic forms of human mannose binding protein. *Nat. Genet.*, **2**, 50-55.

Suzuki, E., Toledo, M. S., Takahashi, H. K. and Straus, A. H. (1997) A monoclonal antibody directed to terminal residue of beta-galactofuranose of a glycolipid antigen isolated from *Paracoccidioides brasiliensis*: cross-reactivity with *Leishmania major* and *Trypanosoma cruzi*. *Glycobiology*, **7**, 463-468.

Suzuki, Y. A., Shin, K. and Lonnerdal, B. (2001) Molecular cloning and functional expression of a human intestinal lactoferrin receptor. *Biochemistry*, **40**, 15771-15779.

Tsuji, S., Uehori, J., Matsumoto, M., Suzuki, Y., Matsuhisa, A., Toyoshima, K. and Seya, T. (2001) Human intelectin is a novel soluble lectin that recognizes galactofuranose in carbohydrate chains of bacterial cell wall. *J. Biol. Chem.*, **276**, 23456-23463.

Wali, A., Morin, P. J., Hough, C. D., Lonardo, F., Seya, T., Carbone, M. and Pass, H. I. (2005) Identification of intelectin overexpression in malignant pleural mesothelioma by serial analysis of gene expression (SAGE). *Lung Cancer*, **48**,19-29.

Wrackmeyer, U., Hansen, G. H., Seya, T. and Danielsen, E. M. (2006) Intelectin: a novel lipid raft-associated protein in the enterocyte brush border. *Biochemistry*, **45**, 9188-9197.

Legends to figures

Figure 1. Western blotting of hITLN-1 and mITLN-1

Recombinant hITLN-1 (*Rec, Human*), recombinant mITLN-1 (*Rec, Mouse*) and intestinal mITLN-1 (*Int, Mouse*) were purified by galactose-Sepharose adsorption, resolved by SDS-PAGE under non-reducing or reducing conditions, and detected by Western blotting as described in "Materials and Methods."

Figure 2. Alignment of amino acid sequences between hITLN-1 and mITLN-1

Deduced amino acid sequences of hITLN-1 and mITLN-1 are shown. The homologous amino acids are shown in *shaded characters*. Cys-31, Cys-48, and Asn-163 in hITLN-1 are shown as *black boxes*. Putative signal peptides of hITLN-1 (Tsuji *et al*., 2001) and mITLN-1 (Komiya *et al*., 1998) are shown as *gray characters*. The *solid line* and the *open line* indicate the N-terminal and C-terminal regions of chimeric molecules between hITLN-1 and mITLN-1. Sequence information was obtained from GenBank database as follows: human ITLN-1, AB036706; mITLN-1, AB016496.

Figure 3. Western blotting of chimeric molecules between hITLN-1 and mITLN-1 and point mutants of hITLN-1

Samples were purified by adsorption to galactose-Sepharose and elution with EDTA. Proteins were resolved by SDS-PAGE under non-reducing or reducing conditions, and detected by Western blotting as described in "Materials and Methods." *Human*, hITLN-1; *Hu/Mo*, Hu/Mo chimeric ITLN-1; *Mo/Hu*, Mo/Hu chimeric ITLN-1; *Mouse*, mITLN-1;

48C>S, 48C>S hITLN-1; *31,48C>S*, 31,48C>S hITLN-1; *31C>S*, 31C>S hITLN-1.

Figure 4. Western blotting of oligosaccharide-deficient hITLN-1 and PNGase-treated hITLN-1 and mITLN-1

Purified hITLN-1 and mITLN-1 were treated with PNGase F, resolved by SDS-PAGE under non-reducing or reducing conditions, and detected by Western blotting as described in "Materials and Methods." *Human*, hITLN-1; *163N>K*, 163N>K hITLN-1; *Human+PNGase*, hITLN-1 treated with PNGase F; *Mouse*, mITLN-1; *Mouse+PNGase*, mITLN-1 treated with PNGase F.

Figure 5. Competitive elution of hITLN-1 and mITLN-1 from galactose-Sepharose

hITLN-1 or mITLN-1 was eluted from galactose-Sepharose with 10 mM EDTA or 100 mM saccharide as described in "Materials and Methods." Values of *density* were determined from the corresponding electropherogram with image analysis software, and represent the relative amount of eluted ITLN-1. *A*; *Gal*, galactose; *2-dGal*, 2-deoxygalactose; *6-dGal*, 6-deoxygalactose (D-fucose); *Lac*, lactose; *Mel*, melibiose; *GalpG*, 2-acetamido-2-deoxy-4-O-beta-D-galactopyranosyl-D-glucopyranose; *GalfG*, 2-acetamido-2-deoxy-4-O-beta-D-galactofuranosyl-D-glucopyranose; *GlcNAc*, N-acetylglucosamine. *B*; *Ara*, arabinose; *Lyx*, lyxose; *Xyl*, xylose; *Rib*, ribose. *C*; hITLN-1 or mITLN-1 in culture supernatants was incubated for 18 h at 4ºC with galactose-Sepharose and various concentrations of galactose, washed with TBS containing 2 mM $CaCl_2$, and eluted with 10 mM EDTA. The binding ratio indicates the percentage of

ITLN-1 bound to galactose-Sepharose compared to the total ITLN-1 bound from culture supernatants without added galactose.

Figure 6. Competitive elution of chimeric molecules and point mutants by galactose-derived saccharides

Each ITLN-1 was eluted from galactose-Sepharose with 10 mM EDTA, 100 mM 2-deoxygalactose (*2-dGal*), or galactose (*Gal*) as described in “Materials and Methods.” Eluted ITLN-1 was subjected to SDS-PAGE and band densities were determined with image analysis software and are expressed as percentage of ITLN-1 eluted with EDTA. *Human*, hITLN-1; *Mouse*, mITLN-1; *Hu/Mo,* Hu/Mo chimeric ITLN-1; *Mo/Hu*, Mo/Hu chimeric ITLN-1; *48C>S*, 48C>S hITLN-1; *31,48C>S*, 31,48C>S hITLN-1.

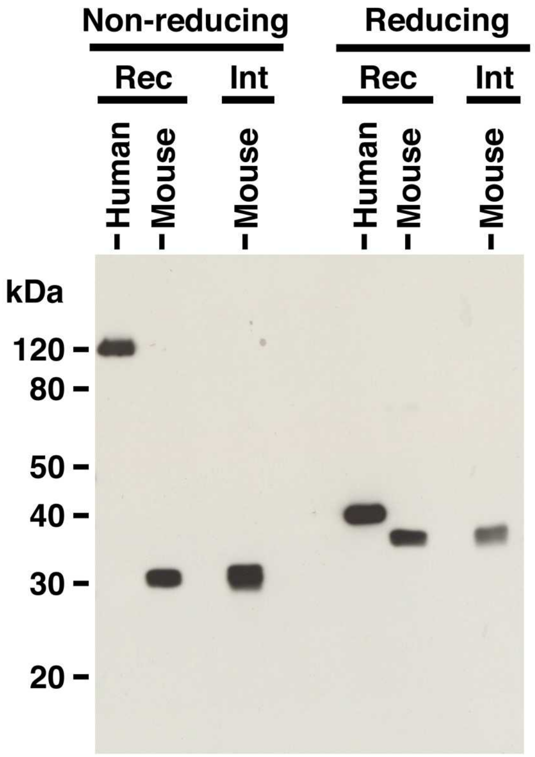
Non-reducing
Reducing
Rec
Int
Rec
Int
Human
Mouse
Mouse
Human
Mouse
Mouse
kDa
120
80
50
40
30
20

Fig. 1

```
                                   31              48
hITLN-1  MNQLSFLLFLIATTRGWSTDEANTYFKEWTCSSSPSLPRSCKEIKDECPSAFDGLYFLRT   60
mITLN-1  MTQLGFLLFIMVATRGCSAAEENLDTNRWGNSFFSSLPRSCKEIKQEHTKAQDGLYFLRT   60

hITLN-1  ENGVIYQTFCDMTSGGGGWTLVASVHENDMRGKCTVGDRWSSQQGSKADYPEGDGNWANY  120
mITLN-1  KNGVIYQTFCDMTTAGGGWTLVASVHENNMRGKCTVGDRWSSQQGNRADYPEGDGNWANY  120

                                                      163
hITLN-1  NTFGSAEAATSDDYKNPGYYDIQAKDLGIWHVPNKSPMQHWRNSSLLRYRTDTGFLQTLG  180
mITLN-1  NTFGSAEAATSDDYKNPGYFDIQAENLGIWHVPNKSPLHNWRKSSLLRYRTFTGFLQHLG  180

hITLN-1  HNLFGIYQKYPVKYGEGKCWTDNGPVIPVVYDFGDAQKTASYYSPYGQREFTAGFVQFRV  240
mITLN-1  HNLFGLYKKYPVKYGEGKCWTDNGPALPVVYDFGDARKTASYYSPSGQREFTAGYVQFRV  240

hITLN-1  FNNERAANALCAGMRVTGCNTEHHCIGGGGYFPEASPQQCGDFSGFDWSGYGTHVGYSSS  300
mITLN-1  FNNERAASALCAGVRVTGCNTEHHCIGGGGFFPEGNPVQCGDFASFDWDGYGTHNGYSSS  300

hITLN-1  REITEAAVLLFYR                                                313
mITLN-1  RKITEAAVLLFYR                                                313
```

Fig. 2

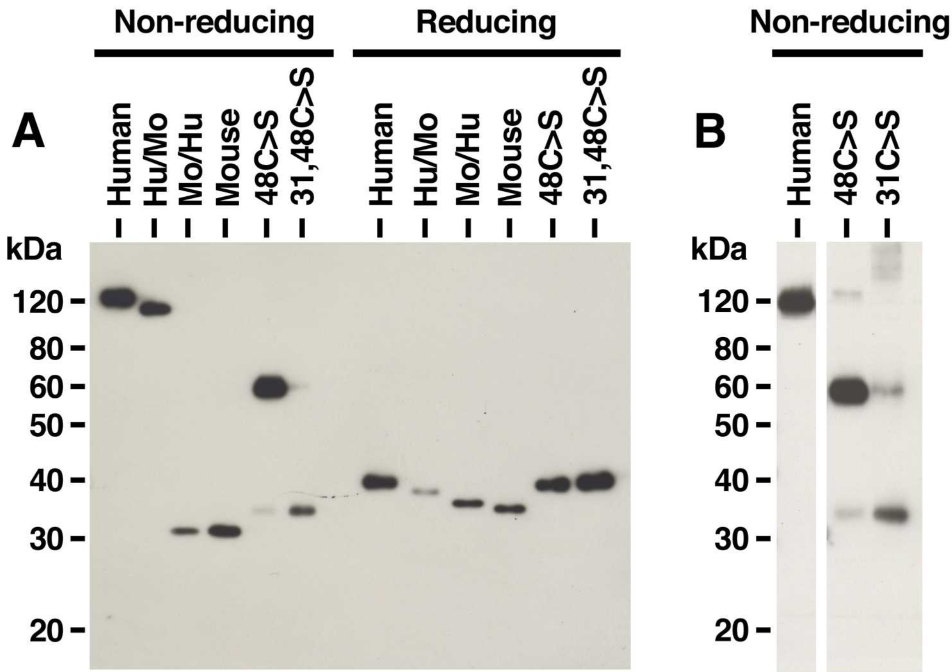
Non-reducing
Reducing
Non-reducing
A
Human
Hu/Mo
Mo/Hu
Mouse
48C>S
31,48C>S
Human
Hu/Mo
Mo/Hu
Mouse
48C>S
31,48C>S
B
Human
48C>S
31C>S
kDa
120
80
60
50
40
30
20
kDa
120
80
60
50
40
30
20

Fig. 3

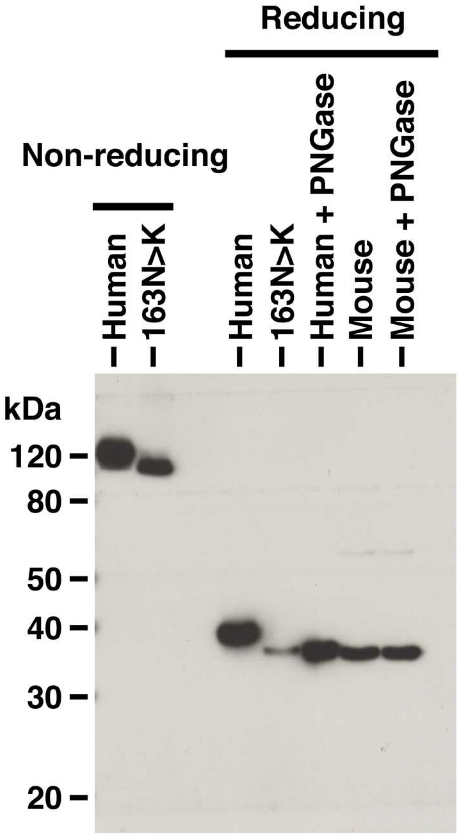
Reducing
Non-reducing
Human
163N>K
Human
163N>K
Human + PNGase
Mouse
Mouse + PNGase
kDa
120
80
50
40
30
20

Fig. 4

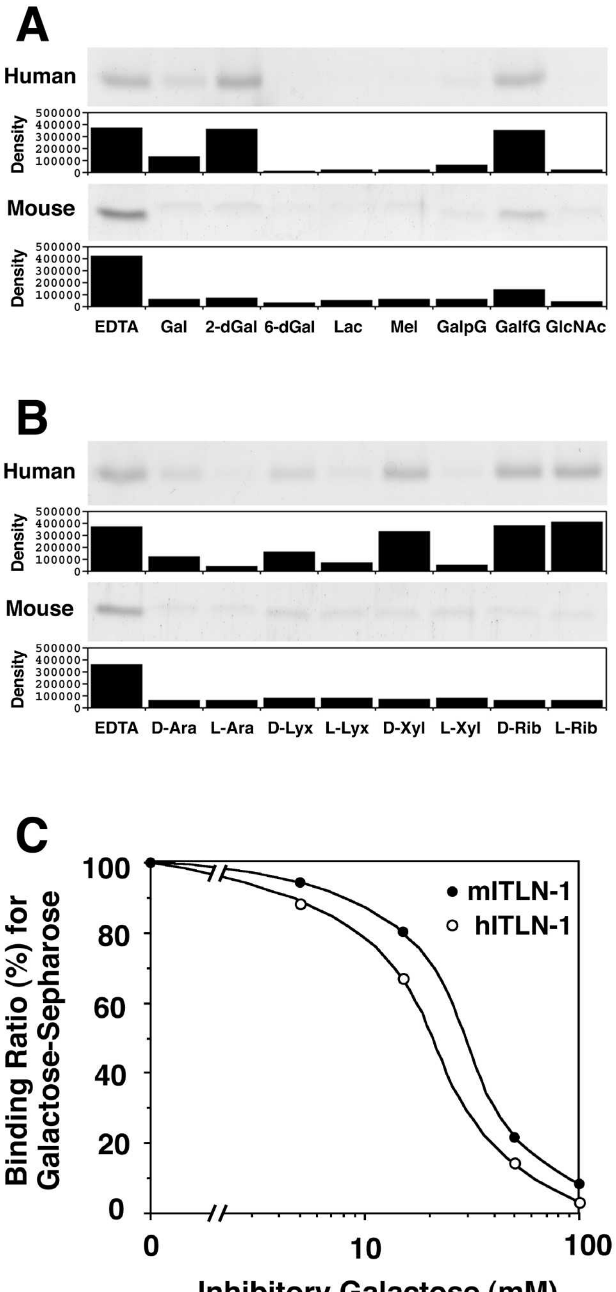
A
Human
Density
500000
400000
300000
200000
100000
0
Mouse
Density
EDTA
Gal
2-dGal
6-dGal
Lac
Mel
GalpG
GalfG
GlcNAc
B
Human
Density
Mouse
Density
EDTA
D-Ara
L-Ara
D-Lyx
L-Lyx
D-Xyl
L-Xyl
D-Rib
L-Rib
C
Binding Ratio (%) for Galactose-Sepharose
100
80
60
40
20
0
mITLN-1
hITLN-1
0
10
100
Inhibitory Galactose (mM)

Fig. 5

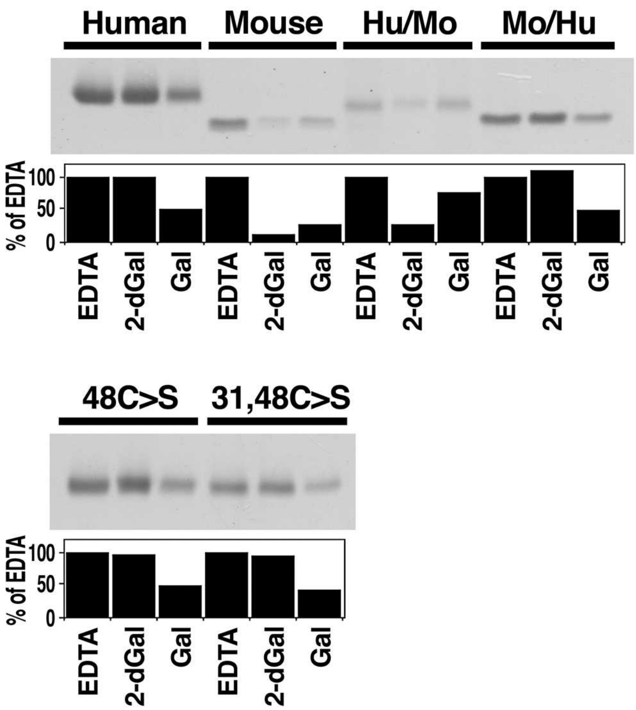
Human
Mouse
Hu/Mo
Mo/Hu
% of EDTA
100
50
0
EDTA
2-dGal
Gal
48C>S
31,48C>S

Fig. 6

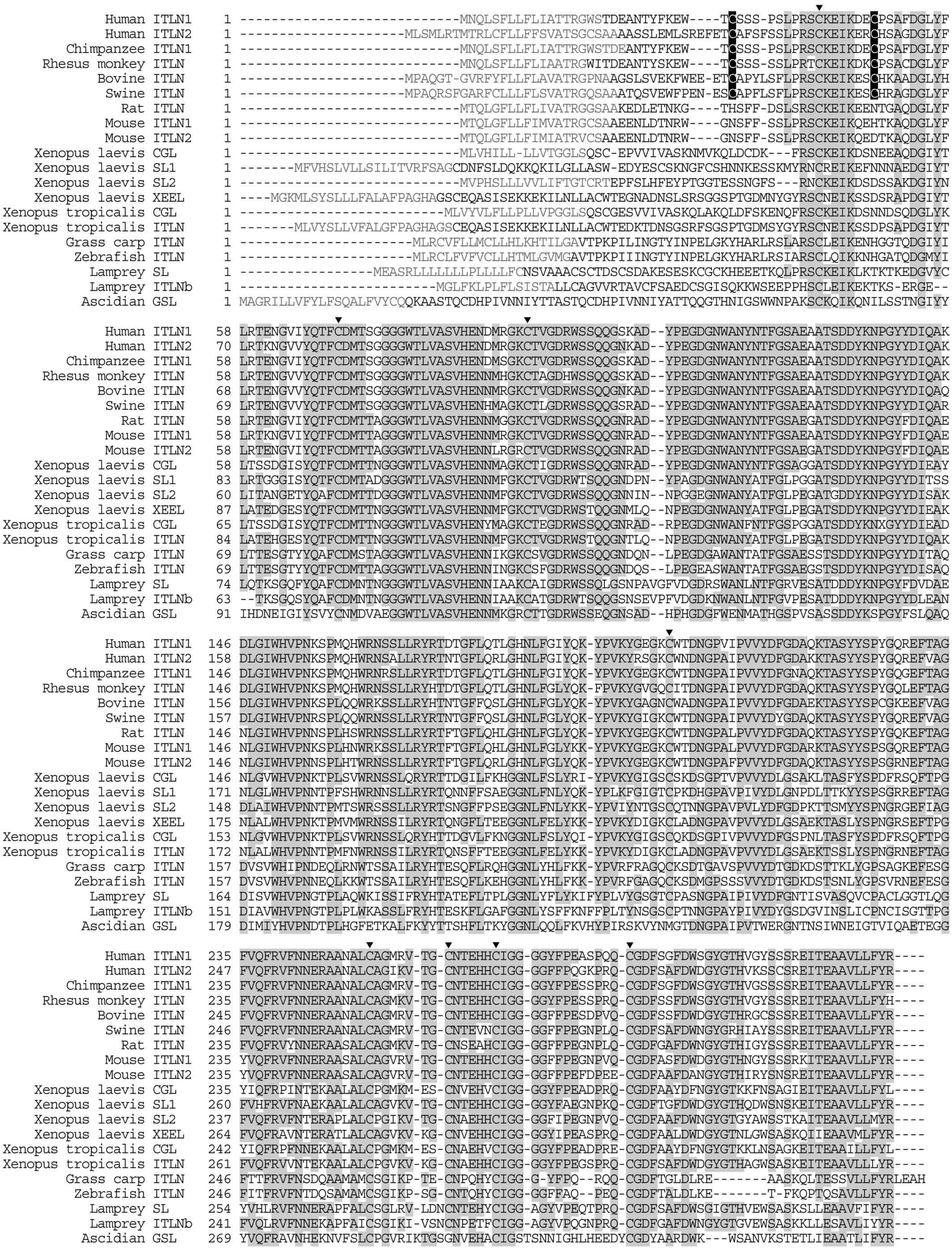

Supplementary Data

Legend to supplementary data

Supplementary data. Alignment of amino acid sequences among ITLN homologues

Deduced amino acid sequences of ITLN homologues are shown. The homologous amino acids are shown in shaded characters. Cys-31 and Cys-48 in hITLN-1 are shown as black boxes, respectively. Highly conserved cysteines are indicated by arrows. Putative signal peptides which were referred from a report of Chang *et al*. (2004), or deduced by GENETYX-MAC are shown as gray characters. Sequence information was obtained from GenBank database or the literature as follows: human ITLN1, AB036706; human ITLN2 (HL-2), NM_080878; chimpanzee ITLN1, XM_513928; rhesus monkey ITLN, XM_001117633; bovine ITLN, CK973402 and CK968253; swine ITLN, BW981762 and DY409179; rat ITLN, NM_001034946; mouse ITLN1, AB016496; mouse ITLN2, NM_001007552; Xenopus laevis CGL (cortical granule lectin), X82626; Xenopus laevis SL1 (35 kDa serum lectin), AB061238; Xenopus laevis SL2 (serum lectin type2), AB061239; Xenopus laevis XEEL, AB105372; Xenopus tropicalis CGL, AY079196; Xenopus tropicalis ITLN, BC061445; grass carp ITLN, DQ020100; zebrafish ITLN, XM_677825; lamprey SL (serum lectin), AB055981; lamprey ITLNb, AB114629; ascidian GSL (galactose-specific lectin), a report of Abe *et al*. (1999).